Received: 13 May 2019 | Revised: 25 August 2020 | Accepted: 26 August 2020

DOI: 10.1111/joa.13313

ORIGINAL PAPER

ANATOMICAL SOCIETY Journal of Anatomy WILEY

Functional Morphology of the Feeding Apparatus of the Snaggletooth Shark, *Hemipristis elongata* (Carcharhiniformes: Hemigaleidae)

Anthony Chappell[1] | **Bernard Séret**[2]

[1]Chondrognatha, Cramoisy, France

[2]IchthyoConsult, Igny, France

Correspondence
Anthony Chappell, Chondrognatha, 2 place de la République, 60660 Cramoisy, France.
Email: chondrognathos@hotmail.fr

Abstract

The anatomy of the feeding apparatus of the snaggletooth shark, *Hemipristis elongata* (Klunzinger, 1871) is illustrated in detail from the dissection of three heads. Two new muscles are described: the *Adductor mandibularis internus* and the *Levator mandibularis*. A subdivision of the *Levator palatoquadrati* is described and named the *Pronator* subdivision of the *Levator palatoquadrati*. Also, eight new anatomical features associated with the mandibular arch and with the chondrocranium (CR) are described. Three are cartilages: the suprapalatine cartilages, the craniopalatoquadrate cartilage and the calcified Meckelian dental fold. The remaining five features are processes: the *Pronator* process of the palatoquadrate (PQ), the *Levator palatoquadrati alpha* process, the proquadrate process, the ectorbital process (ECP) and the Meckelian *Intermandibularis* ridge. Some of them are not restricted to *H. elongata*. The function of these new muscles and anatomical features is discussed and a hypothesis about the functional morphology of the feeding apparatus of the snaggletooth shark is proposed. The extent and the assumptive importance of the pronation of the mandibular arch in the snaggletooth shark feeding behaviour is described and discussed. An alternative for the main function of the *Levator palatoquadrati* as hypothesized by Motta et al. (1997) and Wilga et al. (2001) is proposed for the families Hemigaleidae, Carcharhinidae and Sphyrnidae. We anticipate this muscle is more involved in the pronation rather than in the protrusion of the mandibular arch.

KEYWORDS

Adductor mandibularis internus (new muscle), cephalic anatomy, feeding functional anatomy, *Hemipristis elongata*, *Levator mandibularis* (new muscle), mandibular arch, pronation, suprapalatine cartilages (new)

1 | INTRODUCTION

The snaggletooth shark, *Hemipristis elongata* (Klunzinger, 1871) is a coastal shark widely distributed in the Indo-West Pacific, Indian Ocean and the Red Sea (Compagno, 1984; Ebert et al., 2013). It occurs from the sea surface to at least 132-m deep and is known to live inshore and offshore above the continental shelf and slope. Although not commonly reported (111 records in the biodiversity database GBIF with only 47 specimens preserved in collections), it seems that this shark could be relatively common in some areas where it is regularly caught in fisheries in India, Thailand (Sirachai Arunrugstichai, pers. com.), Indonesia and northern Australia. Several molecular studies propose different phylogenetic trees for sharks; the phylogeny tree proposed by Velez-Zuazo & Argnasson

(2011) suggests the family Hemigaleidae is paraphyletic with *Chaenogaleus* +Hemigaleus separated from *Hemipristis*, the latter being surprisingly the sister taxon of *Leptocharias*. Furthermore, this phylogeny does not include the genus *Paragaleus*. In the present work, we followed the phylogeny proposed online by G. Naylor, as it is completed, continuously updated and largely adopted by chondrichthyan scientists.

According to Naylor et al. (Chondrichthyan Tree of Life, https://sharksrays.org/ consulted in March 2020), *Hemipristis elongata* is the sister taxon of all other hemigaleid genera: *Paragaleus*, *Chaenogaleus* and *Hemigaleus* (Figure 1). The hemigaleids are the sister group of *Galeocerdo*, carcharhinoids and sphyrnids. The family Hemigaleidae comprises eight species that are small demersal sharks (Max TL: 90-150 cm) living in inshore waters, mostly in the Indo-West Pacific, with a species in the eastern central Atlantic. The snaggletooth shark is larger than the other Hemigaleids (Max. TL: 240 cm), it is also demersal but both inshore and offshore (Ebert et al., 2013).

Hemipristis elongata feeding apparatus has been little studied; the most extensive surveys of the anatomy and morphology of this shark are provided by Baranes et al. (1979), Compagno (1988), and Smith (1957). The cranial morphology, head anatomy and feeding mechanisms have been documented for *Negaprion brevirostris* (Frazzetta, 1994; Motta & Wilga, 1995; Motta et al., 1997; Poey, 1868) and for *Carcharhinus limbatus* (Valenciennes, 1839; Huber et al., 2006 and Motta & Huber, 2012) within carcharhinoids. The cephalic musculature of various higher carcharhinoids encompassing the families Hemigaleidae, Carcharhinidae and Sphyrnidae (Sensu Compagno, 1988), including a Hemigaleid (*Paragaleus* sp.), has been illustrated by Compagno (1988) and by Soares & Carvalho (2013). Finally, the bonnethead shark, *Sphyrna tiburo* (Linnaeus, 1758), is the only sphyrnid shark that has been investigated regarding its cephalic anatomy and feeding mechanics (Mara et al., 2009; Wilga & Motta, 2000). This present paper provides the first study dedicated to cephalic anatomy for a hemigaleid shark. The aims were: (a) to describe the morphology of the feeding apparatus of the snaggletooth shark to provide a comprehensive anatomical review of its myological, tendinous, ligamentous and cartilaginous structures; (b) to infer a feeding mechanism in developing the concept of mandibular arch pronation within Hemigaleidae; and (c) to propose a new theory regarding the function of the *Levator palatoquadrati* in the higher carcharhinoids.

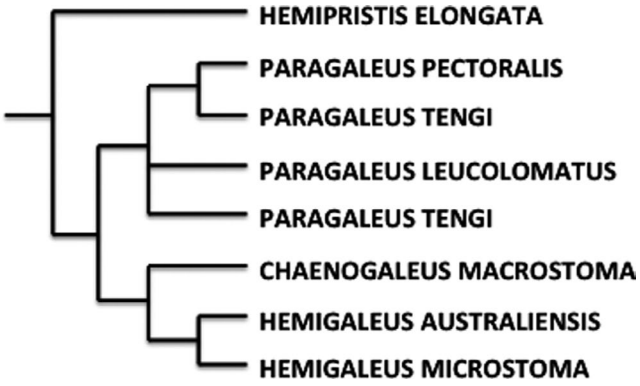

FIGURE 1 Phylogenetic relationships of the Hemigaleidae After Naylor et al. (Chondrichthyan Tree of Life, https://sharksrays.org/, consulted in March 2020)

2 | MATERIALS AND METHODS

The heads were removed from two specimens of *H. elongata* from the Seychelles Islands. A 1787-mm TL mature male caught off Mahé on 16 October 2011 is illustrated in Figure 2. A 1260-mm TL male whose level of maturity has not been ascertained was caught off Mahé on August 2014. The third head was removed from a 1920-mm TL mature male caught in the shark nets at Umgababa, Natal, South Africa. These specimens were provided to the authors for dissection and were received either frozen or salted. No noticeable differences were observed between the salted and the frozen heads once those were properly defrosted and desalted. The functional morphology and kinematics regarding *H. elongata* were inferred from these three heads only.

An additional set of six dried jaws from *H. elongata* specimens (from about 800 to 2350-mm TL) collected from the Philippines, Gulf of Thailand and South Madagascar were also taken into account in this study. The drying process of the jaws of the snaggletooth shark barely affects or deforms the cartilages as the authors noted in comparing this material with the desalted and defrosted dissected specimens. These jaws were used as comparative material on an anatomical level only. They were obtained by the senior author from collectors'network and were properly identified.

Comparative material includes two heads of *Hemigaleus australiensis* (White, Last and Compagno, 2005) that were removed from specimens caught in Papua New Guinea. This material was not sexed nor measured. These salted heads were provided to the authors for dissection. Additional comparative material included dried jaws from *Chaenogaleus macrostoma* (Bleeker, 1852), *Hemigaleus microstoma* (Bleeker, 1852), *Paragaleus pectoralis* (Garman, 1906) and *P. randalli* (Compagno, Krupp and Carpenter, 1996). These hemigaleid shark jaws were obtained by the senior author from collectors'network and were properly identified. This material comprises all the genera belonging to the same family as the snaggletooth shark: the Hemigaleidae (Hasse, 1879). They were used for anatomical comparisons with the mandibular arch of *H. elongata*. A frozen immature 470-mm TL female *Carcharhinus melanopterus* (Quoy & Gaymard, 1824),

FIGURE 2 *Hemipristis elongata*, male of 1787-mm TL, from the Seychelles Islands. Yellow ruler is 160 cm long. Photo B.S

and the frozen head of a 1720-mm TL adolescent female *Sphyrna lewini* (Griffith and Smith, 1834) were donated by a public aquarium. They were used for dissection and comparison with the *H. elongata* material. Articulated and fresh complete skulls of the following Lamnoid taxa were also used as comparative material: *Isurus oxyrinchus* (Rafinesque, 1810), *Lamna nasus* (Bonnaterre, 1788), *Carcharias taurus* (Rafinesque, 1810) and *Mitsukurina owstoni* (Jordan, 1898). These specimens were obtained from fish markets or donated to the authors. Dry chondrocrania of adult *L. nasus*, *C. taurus* and *I. oxyrinchus* were also used for comparison with the *H. elongata* skull. Dried jaws of *Carcharodon carcharias* (Linnaeus, 1758), *Isurus* (Rafinesque, 1810), *Lamna* (Cuvier, 1817), *Odontaspis* (Risso, 1810), *C. taurus*, *M. owstoni*, *Alopias* (Rafinesque, 1810) *and Pseudocarcharias kamoharai* (Matsubara, 1936) were used for comparison with *H. elongata* on an anatomical level only. This material was obtained from fish markets, collectors'network or has been donated to the senior author.

Prior to investigation, the salted heads of *H. elongata* and *H. australiensis* were washed in successive baths of tap water for about 12 hours. These heads were drained and eventually frozen. The frozen heads of *H. elongata*, *H. australiensis*, *C. melanopterus* and *S. lewini* were defrosted in tap water. The three *H. elongata* heads were carefully dissected in order to reveal their myological, cartilaginous, tendinous and ligamentary structures. At every step of the dissections, photographs were taken from chosen axes. Illustrations were drawn after the observations and manipulations of the fresh specimens. The drawings were based on photographs using tracing paper to render as accurate as possible all details of the relevant anatomical features (Figure 7d,e). The two heads of *H. australiensis* underwent the same investigating process. The *C. melanopterus* underwent a similar process for the *Levator palatoquadrati* only. The *S. lewini* head was dissected and its structures compared to those of *H. elongata*. Observations resulting from manipulations of fresh complete and skeletonized *I. oxyrinchus*, *C. taurus and M. owstoni* heads were taken into account. These observations were compared with *H. elongata* regarding their mandibular arch pronation abilities (Unpublished observations).

Only hand manipulations could provide relevant information about biomechanics in our *H. elongata* material. Once the three heads were thawed, we readily noted the ease with which the pronation of the mandibular arch was achieved. Subsequently, these hand manipulations were performed once the heads were devoid of skin and more particularly with completely skeletonized specimens and their ligaments. The degree of articular amplitude and its limitation were empirically assessed by the first sign of resistance for each articulation joint stop. This rule was particularly decisive for the pronation and abduction limit assessment of the mandibular arch in the *H. elongata*, *H. australiensis* and *C. melanopterus* skeletonized specimens. Frazetta described an external rotation of the PQ on a longitudinal double jaw joint—upper symphysis axis he named "longitudinal rotation of the jaws" (Frazetta, 1994, p.45). Scott (2016) in his Master thesis retained his concept and named it "pronation." In some studies dealing with jaw kinematics of higher vertebrates, such as carnivorous mammals, the term "eversion" and "inversion" are used to describe the longitudinal rotation of the mandibula (e.g. Bhullar et al., 2019). Although these terms could be applied to the kinematics of the jaws of *Hemipristis*, we think it is more judicious to keep the terms proposed by Scott, 2016 for sharks, for consistency.

In human biomechanics, the term pronation defines the rotation of the forearm and the hands so that the palm faces backwards or downwards. At the opposite, the term supination is the rotation of the forearm and hand so that the palm faces forward or upward. These terms were generally applied to shark jaw biomechanics by Scott (2016) to describe the feeding kinematics of the white-spotted bamboo shark *Chiloscyllium plagiosum* (Bennett, 1830). The pronation of the mandibular arch is expressed when the dorsal rim of the PQ rotates medially on a double jaw joint—upper symphysis longitudinal axis, concomitantly with its ventral rim rotating laterally and externally. Likewise, the Meckel's cartilage (MC) pronates when its dorsal tooth-bearing margin rotates medially on a double jaw joint—lower symphysis longitudinal axis while its ventral rim rotates laterally and externally (Figures 3, 5a,b,c and 9a,b).

Terminologies and abbreviations for cartilages, muscles, ligaments and teeth follow: Compagno (1988), Shirai (1992), Wilga (1995), Motta (1995), Goto (2001), Wilga (2005) and Huber et al. (2011) with additions and modifications from the authors.

3 | RESULTS

3.1 | Description of the dentition

The dentition of the three *H. elongata* specimens complies with the description found in the literature in terms of morphology, arrangement and meristic (Baranes et al., 1979; Bass et al., 1975; Compagno, 1988; Fourmanoir, 1961; Herman et al., 2003; Leriche, 1938; Smith, 1957).

The upper teeth are larger and more compressed labiolingually than the lower. They are semi-crescentic in shape, and strongly serrated on both edges in subadults and adults. The mesial edge is smooth in juveniles. They are tightly overlapping in an imbricate/alternate fashion on one, rarely two functional rows along the upper jaw (Compagno, 1988). The three to four first files on each side of the symphysis are narrower and their crowns are more lingually curved than the lateroposterior ones. They are often arranged with a supernumerary functional row. The subsequent files display teeth with crowns that are flat or slightly curved labially. The teeth of the anterior files markedly protrude labially compared to the subsequent ones. The monognathic heterodonty is gradual along the jaw margin. It is expressed by a reduction in size from the sixth tooth to the commissural one. The anterior teeth within the dental bulla display a more accentuated gradual heterodonty with the two first being narrow, small and smooth edged. There is a toothless space at the symphysis.

The lower teeth are much more narrow and their crowns are more lingually curved than the uppers. The anterior teeth are hooked and are strongly protruding labially. The monognathic heterodonty is gradual but is very pronounced along the tooth files. The anterior teeth

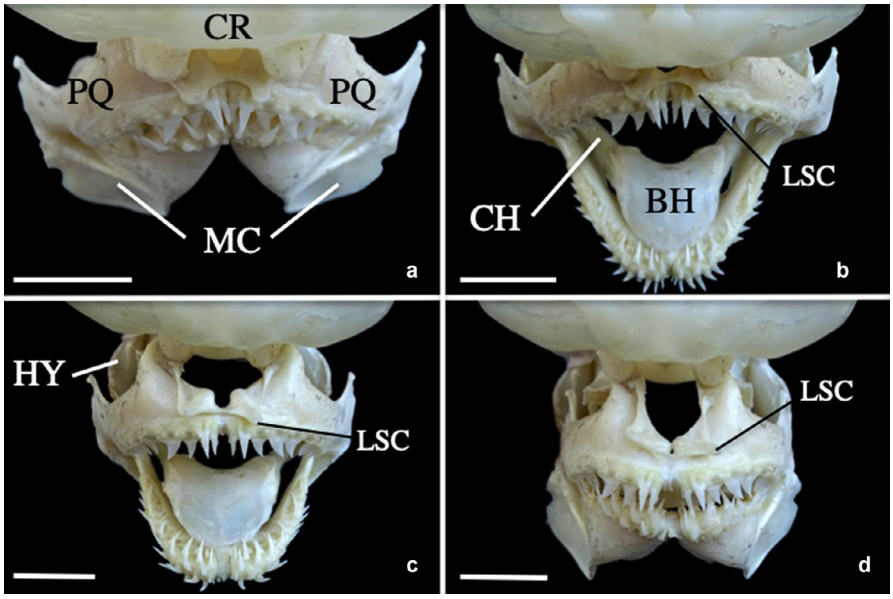

FIGURE 3 Demonstration of pronation ability of the *Hemipristis elongata* mandibular arch induced by hand manipulation (1260-mm TL specimen). Frontal view. (a) mouth closed and mandibular arch braced against the chondrocranium. (b) lower jaw depressed initiating mandibular arch pronation. (c) onset of adduction and protrusion of the mandibular arch. (d) mandibular arch with adduction, protrusion and pronation fully completed. Black arrow points the distal end of the left LSC. BH, basihyal; CH, ceratohyal; CR, chondrocranium; HY, hyomandibula; LSC, lower suprapalatine cartilage; MC, Meckel's cartilage; PQ, palatoquadrate. Scale bar is 2 cm. Photograph A.C

are long, very narrow and mostly smooth edged. The monognathic heterodonty is expressed by the shortening and the straightening of the crown as well as by the addition of cusps along the cutting edges, particularly on the distal one. There are usually two functional rows along the jaw margins. There is a toothless space at the symphysis.

3.2 | Description of the chondrocranium

The CR of *H. elongata* displays the features of higher carcharhinoids (Hemigaleidae, Carcharhinidae and Sphyrnidae) such as the lack of supraorbital crests, the presence of high and thick ectethmoid condyles (ECNs) and separated nasal apertures and fontanelles (Compagno, 1988). It displays the additional relevant following structures that are absent or weakly developed in other higher carcharhinoids:

3.2.1 | Subethmoid keel (Medial keel of Compagno, 1988; SK)

The subethmoid fossa is longitudinally cleft by a high, strong and compressed keel. This keel originates from the internasal septum where it is the tallest. It gently slopes posteriorly to merge into the basal plate (BP) at the level of the orbital notches (NPs). This keel is barely developed in *H. australiensis* and is absent in *C. melanopterus*. It is developed in various stages of shape and extent in *Lamiopsis* (Gill, 1862), *N. brevirostris*, *Isogomphodon oxyrhynchus* (Muller and Henle, 1839) and as well as in various *Carcharhinus* spp. (*C. obscurus*; LeSueur, 1818; in Compagno, 1988 and *C. limbatus*, unpublished observations). In these taxa, however, it is not as high or as compressed as in *H. elongata*. Some lamnoids develop a similar keel (*C. taurus*; *Alopias pelagicus*, Nakamura, 1935; Compagno, 1990; present study) (Figures 4b,c and 6b).

3.2.2 | Basal plate keel (BPK)

The rear part of the BP developed a strong median triangular keel. This keel rises from the middle of the BP and is flanked by deep *Epaxial* muscle fossae (EPM). The keel begins to taper anterior to the lateral aortic foramina (LAF) and fails to reach the occipital hemicentrum (OHC). A similar keel is blunt and flat in *H. australiensis* and does not split the posterior area of the BP. It is known in *C. macrostoma* and *Galeocerdo* (Muller and Henle, 1837) as well as in some *Sphyrna* (Rafinesque, 1810) and *Rhizoprionodon* (Compagno, 1988; Ruppell, 1837). In *C. melanopterus*, there is, in this area, a very low and blunt longitudinal bulge flanked by the otic capsules (OTs). Many lamnoid taxa develop a similar condition to *H. elongata* (*Lamna*,Cuvier, 1817; *Isurus* (Rafinesque, 1810); *Odontaspis ferox* (Risso, 1810); Compagno, 1990; present study) Figure 4b.

3.2.3 | Basal plate *Epaxial* fossae (EPM)

The BP behind the NPs is ventrolaterally arched and concave dorsally. The suborbital shelves are lateroventrally oriented (SS; Figure 4b,c). The lower portion of the *Epaxial* inserts in between these arched suborbital shelves and the BPK. The extreme posterolateral end of the BP exhibits a strong and roughly triangular vertical depression; the basal plate depression (BPD; Figure 4b). This

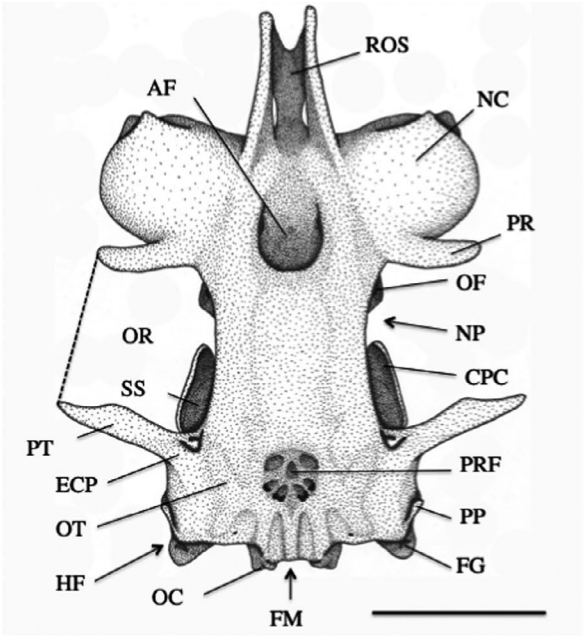

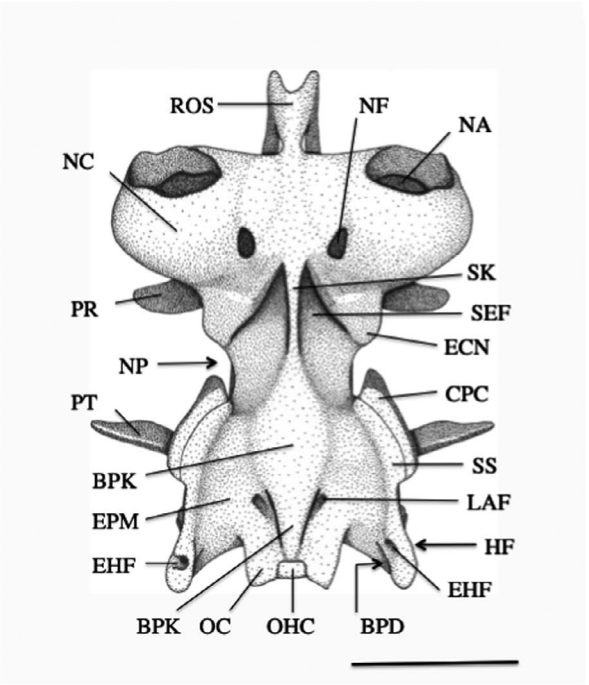

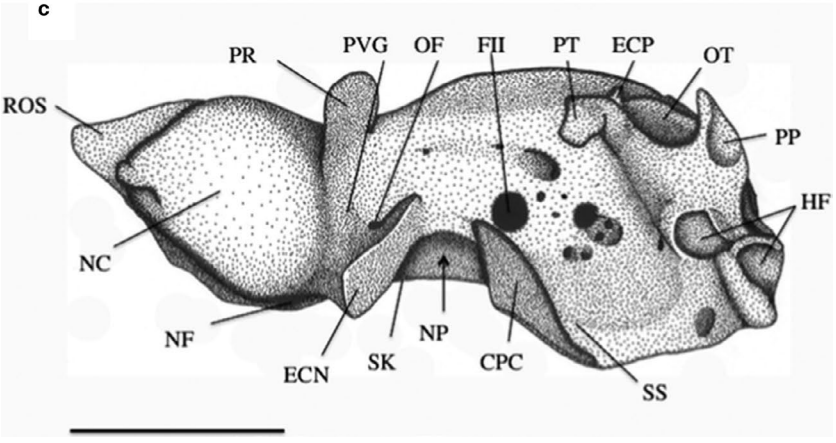

FIGURE 4 (a) Dorsal view of the chondrocranium of *Hemipristis elongata* (1787-mm TL specimen). AF, anterior fontanelle; CPC, craniopalatoquadrate cartilage; ECP, ectorbital process; FG, glossopharyngeal nerve foramen; FM, foramen magnum; NC, nasal capsule; NP, orbital notch; OC, occipital condyle; OF, orbitonasal foramen; OR, orbit; OT, otic capsule; PP, pterotic process; PR, preorbital process; PRF, parietal fossa; PT, postorbital process; ROS, rostral cartilages; SS, suborbital shelf. Scale bar is 5 cm. Drawing A.C. (b) Ventral view of the chondrocranium of *Hemipristis elongata* (1787-mm TL specimen). BP, basal plate; BPD, basal plate depression; BPK, basal plate keel; CPC, craniopalatoquadrate cartilage; ECN, ectethmoid condyle; EHF, efferent hyoidian foramen; EPM, *Epaxial* muscle fossa; HF, hyomandibular fossa; LAF, lateral aortic foramen; NA, nasal aperture; NC, nasal capsule; NF, nasal fontanelle; NP, orbital notch; OC, occipital condyle; OHC, occipital hemicentrum; PR, preorbital process; PT, postorbital process; ROS, rostral cartilages; SEF, subethmoid fossa; SK, subethmoid keel; SS, suborbital shelf. Scale bar is 5 cm. Drawing A.C. (c) Lateral view of the chondrocranium of *Hemipristis elongata* (1787-mm TL specimen). CPC, craniopalatoquadrate cartilage; ECN, ectethmoid condyle; ECP, ectorbital process; fII, optic nerve foramen; HF, hyomandibular fossa; NC, nasal capsule; NF, nasal fontanelle; NP, orbital notch; OF, orbitonasal foramen; OT, otic capsule; PP, preorbital process; PR, preorbital process; PVG, ventral *Preorbitalis* groove; ROS, rostral cartilages; SS, suborbital shelf. Scale bar is 5 cm. Drawing A.C

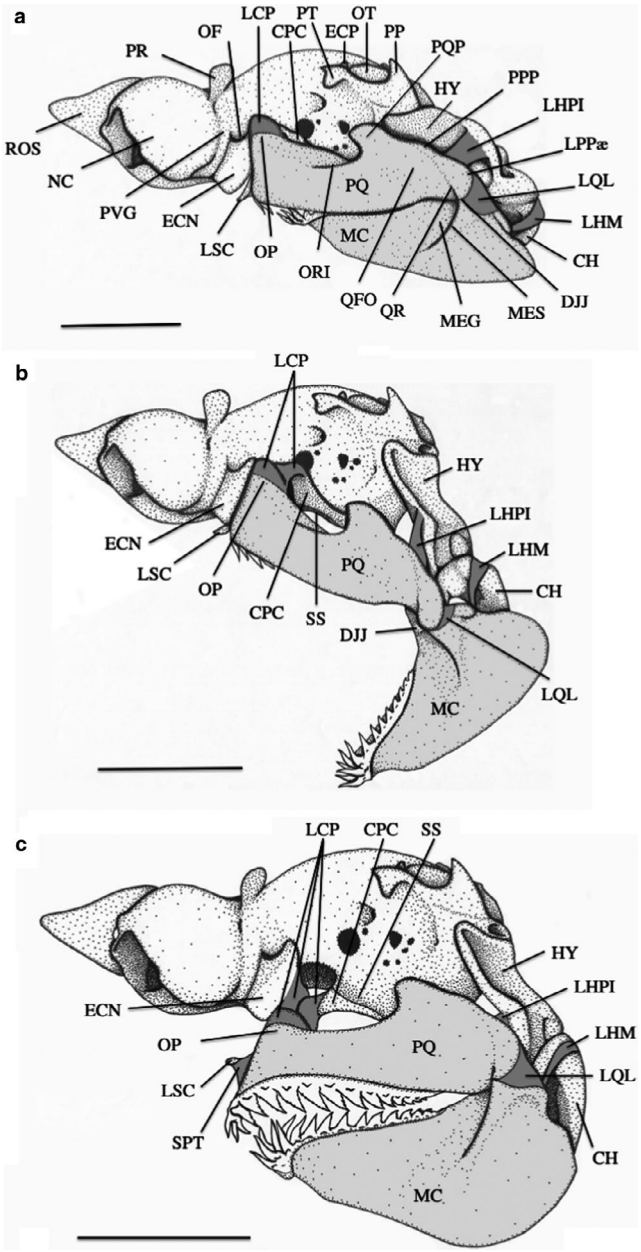

FIGURE 5 (a) Lateral left view of the feeding apparatus of *Hemipristis elongata* (1260-mm TL specimen). The mandibular and hyoid arches are against the chondrocranium and the mouth is closed. CH, ceratohyal; CPC, craniopalatoquadrate cartilage; DJJ, double jaw joint; ECN, ectethmoid condyle; ECP, ectorbital process; HY, hyomandibula; LCP, ethmopalatine ligament; LHM, hyoid-mandibular ligament; LHPI, hyomandibular-palatoquadrate ligament; LPPae, *Levator palatoquadrati* process alpha, LQL, lateral quadratomandibular joint ligament; LSC, lower suprapalatine cartilage; MC, Meckel's cartilage; MEG, Meckelian groove; MES, Meckelian spine; NC, nasal capsule; OF, orbitonasal foramen; OP, orbital process; ORI, orbitoquadrate bridge; OT, otic capsule; PR, preorbital process; PP, postorbital process; PPP, *Pronator* process of the palatoquadrate PQ, palatoquadrate; PQP, proquadrate process; PVG, ventral *Preorbitalis* groove; QFO, quadrate fossa; QR, quadrate ridge; ROS, rostral cartilages. Scale bar is 5 cm. Drawing A.C. (b) Lateral left view of the feeding apparatus of *Hemipristis elongata* (1260-mm TL specimen). The lower jaw is abducted; the mandibular and hyoid arches are depressed. CH, ceratohyal; CPC, craniopalatoquadrate cartilage; DJJ, double jaw joint; ECN, ectethmoid condyle; HY, hyomandibula; LCP, ethmopalatine ligament; LHM, hyoid-mandibular ligament; LHPI, hyomandibular-palatoquadrate ligament; LQL, lateral quadratomandibular jaw ligament; LSC, lower suprapalatine cartilage; MC, Meckel's cartilage; OP, orbital process; PQ; palatoquadrate. Scale bar is 5 cm. Drawing A.C. (c) Lateral left view of the feeding apparatus of *Hemipristis elongata* (1260-mm TL specimen). The mandibular arch is fully protracted and pronated. The mouth is closed. CH, ceratohyal; CPC, craniopalatoquadrate cartilage; ECN, ectethmoid condyle; HY, hyomandibula; LCP, ethmopalatine ligament; LHM, hyoid-mandibular ligament; LHPI, hyomandibular-palatoquadrate ligament; LQL, lateral quadratomandibular joint ligament; LSC, lower suprapalatine cartilage; MC, Meckel's cartilage; OP, orbital process; PQ, palatoquadrate; SPT, suprapalatine cartilage connective tissue; SS, suborbital shelf. Scale bar is 5 cm. Drawing A.C

depression is located just behind the efferent hyoidian artery foramen (EHF). It occurs at the opposite side of the hyomandibular fossa (HF). Some sphyrnids spp. display a similar arched condition of the BP (Compagno, 1988; present study). The suborbital shelves are laterally directed in *H. australiensis* and *C. melanopterus* and their BPD is barely present. In those latter species the *Epaxial* does not extend anteriorly as far as in *H. elongata*. Many lamnoids taxa develop a similar condition to *H. elongata*, with strongly arched BPD and deep BPD (Lamnidae, Alopiidae, Pseudocarchariidae, Odontaspididae; Compagno, 1990; present study). In *H. elongata*, the EHF are shifted to the extreme posterior end of the BP. This is a unique condition among the higher carcharhinoids (note the asymmetrical positioning of these foramina and the length difference of both EPM in Figure 4b). These foramina are located at the level of the anterior margin of the HF in *H. australiensis* as in the other hemigaleid taxa (Compagno, 1988) Figure 4b.

3.2.4 | Pterotic process (PP)

The posterolateral margins of the OTs develop very high, half-crescent and laterally compressed PPs. The PPs occur in *H. australiensis* but are far much less developed. *P. pectoralis* seems not to exhibit such structure (Compagno, 1988). It occurs in the higher carcharhinoids *Galeocerdo*, *Prionace* (Linnaeus, 1758) and the sphyrnids (Compagno, 1988; present study). Many lamnoid taxa possess PPs that are more conical in shape (Lamnidae, Odontaspididae, Pseudocarchariidae, Cetorhinidae; Compagno, 1990; present study) Figure 4a,c.

3.2.5 | Ectorbital process (ECP, newly described structure)

The anterior base of the postorbital process (PT) develops a roughly conical process emerging perpendicularly from it. This structure has never been described before. Compagno did not describe, nor illustrate it (Compagno, 1988; fig. 18.7). This process was present in our three *H. elongata* specimens and seems to be a unique feature of this taxon. *H. australiensis* lacks this process Figure 4a,c.

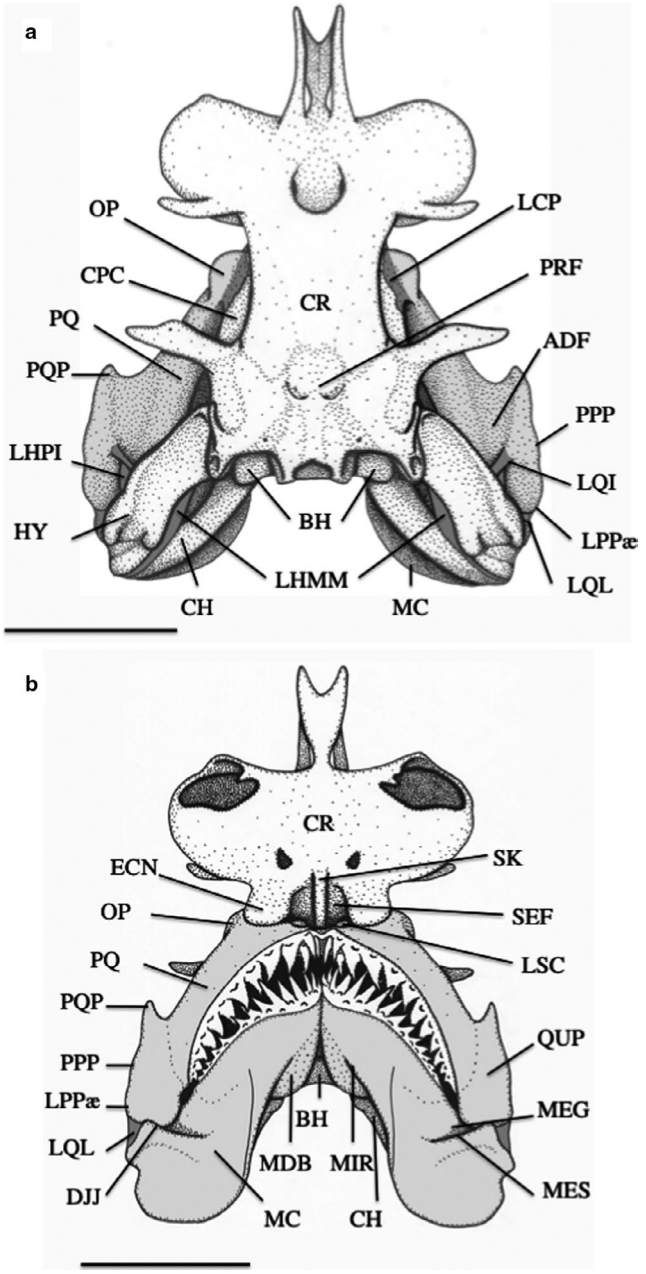

FIGURE 6 (a) Dorsal view of the head skeleton of *Hemipristis elongata* (1787-mm TL specimen). The mandibular and hyoid arches are against the chondrocranium and the mouth is closed. ADF, *Adductor mandibularis internus* fossa; BH, basihyal; CH, ceratohyal; CPC, craniopalatoquadrate cartilage; CR, chondrocranium; HY, hyomandibula; LCP, ethmopalatine ligament; LHMM, medial hyoid-mandibular ligament; LHPI, hyomandibular-palatoquadrate ligament; LPPae, *Levator palatoquadrati* process alpha; LQI, inner *Quadratomandibularis* ligament; LQL, lateral quadratomandibular joint ligament; MC, Meckel's cartilage; OP, orbital process; PPP, *Pronator* process of the palatoquadrate; PRF, parietal fossa; PQ, palatoquadrate; PQP, proquadrate process. Scale bar is 5 cm. Drawing A.C. (b) Ventral view of the head skeleton of *Hemipristis elongata* (1787-mm TL specimen). The mandibular and hyoid arches are against the chondrocranium and the mouth is closed. BH, basihyal; CH, ceratohyal; CR, chondrocranium; DJJ, double jaw joint; ECN, ectethmoid condyle; LPPae, *Levator palatoquadrati* process alpha; LQL, lateral quadratomandibular jaw ligament; LSC, lower suprapalatine cartilage; MC, Meckel's cartilage; MDB, Meckelian dental bulla; MEG, Meckelian groove; MES, Meckelian spine; MIR, Meckelian *Intermandibularis* ridge; OP, orbital process; PPP, *Pronator* process of the palatoquadrate; PQ, palatoquadrate; PQP, proquadrate process; QUP, quadrate process; SEF, subethmoid fossa; SK, subethmoid keel. Scale bar is 5 cm. Drawing A.C

3.2.6 | Craniopalatoquadrate cartilage (CPC, newly described structure)

This ill-calcified, flat and very soft cartilage binds the anterolateral rim of the suborbital shelf (SS) to the orbital process (OP) via a very short ethmopalatine ligament (LCP). This cartilage is present but is very short in *H. australiensis*. It is absent in *C. melanopterus* and *S. lewini*. This cartilage is possibly the calcified homologue of the posterior part of the bifid ethmopalatine ligament that occurs in higher carcharhinoid taxa Figures 4a–c, 5b,c and 6a.

3.2.7 | Hyomandibular fossa (HF)

This depression is borne by a rearward projection of the CR where both EHF and glossopharyngeal foramen (FG) emerge. This rearward extension of the CR is absent among Hemigaleidae and seems to be developed only by some *Sphyrna* spp. (Compagno, 1988; Figure 4a–c).

3.3 | Description of the mandibular arch

3.3.1 | Palatoquadrate

The PQ of *H. elongata* displays the following relevant features:

The PQ dental matrix (PDM) is hyper-developed and inflated. It virtually engulfs the orbital process (OP; Figures 5a and 10a). This condition seems to be related to the massive upper dentition developed and housed in the tooth matrix.

The symphysis is short and is hinged ventrally (Figure 3). There is a short and thick symphyseal ligament. The anteromedial end of each PQ is septate. Each PQ is independent from its antimere and there is a toothless space at the symphysis (Figures 3, 6b and 9b). Macrophageous lamnoids, except *Alopias*, display an analogous condition as in *H. elongata* (present study).

The palatine portion of the PQ forms a dental bulla that houses the four first tooth files (PBU; Figures 9a and 10a). The teeth included in the dental bulla are noticeably narrower than the subsequent lateroposterior teeth. This palatine bulla is absent in *H. microstoma* and *C. melanopterus*. Macrophageous lamnoids develop dental bullae, yet they house the largest teeth of the upper jaw (Shimada, 2002; present study).

There are two pairs of small articulated cartilages embedded in dense connective tissue (SPT) that are located on the mesial half of the palatine portions (PPO). These cartilages are herein named

'upper and lower suprapalatine cartilages' (USCs and LSCs, new structures; Figures 3, 5a–c, 6b, and 9a,b). The shorter upper suprapalatine cartilages (USCs) are tightly articulating with the palatine parasymphyseal ridges (PAR; Figure 10a). The longer lower suprapalatine cartilages (LSCs) are merely lying onto the labial surface of the PQs (Figures 3, 5a and 9a). *H. australiensis* develops a single pair of small, flat and rounded suprapalatine cartilages (SPCs). These small cartilages are embedded in the SPT and do not articulate directly with the palatine portions of the PQs (Figure 11b,e). These structures have never been described hitherto for any sharks. Among elasmobranchs, there are several cartilaginous features that are related to the palatine portions of the PQ. A wide trapezoidal basipalatine cartilage occurs in *Stegostoma (*Muller and Henle, 1837; 'accessory cartilage of palatoquadrate' of Goto, 2001) and a quite smaller and more rounded cartilage is developed in *Nebrius ferrugineus* (Lesson, 1831) and *Ginglymostoma* (Muller and Henle, 1837; pers. observations). The function of this cartilage wedged between the PQs at the posterior end of the palatine symphysis (PSY) is thought to provide additional growth area for symphyseal or parasymphyseal teeth rows. A similar rounded cartilage occurs in at least three species of the *Carcharhinus dussumieri-sealei* group (pers. observations). Its positioning is more offset forward compared to the process found in orectoloboids and it is straightened up. In *Carcharhinus*, the exact function of this cartilage is unknown as of yet. *Dalatias licha* (Bonnaterre, 1788) develops an inverted cap visor-shaped SPC ('symphyseal plate on palatoquadrate' of Shirai, 1992). Its actual function is not clear, either it accommodates with the upper labial cartilages complex or it provides a cushioning function between the PQs and the CR. Among Lamniformes, the Alopiidae and Lamnidae develop a single rod-like cartilage within the palatonasal ligament (Wilga, 2005). Since *H. elongata* does not develop a palatonasal ligament and its SPCs are linked to the ethmopalatine ligaments, we do not consider the rod-like cartilage of the Lamniformes as being homologous to the *H. elongata* condition neither are the extra cartilages of *Stegostoma*, *Ginglymostoma*, *Nebrius*, *Carcharhinus* and *Dalatias*. The rod-like cartilage strengthens the palatonasal ligament in alopiids and lamnids (Wilga, 2005) while the SPCs in *H. elongata* have a hypothetical different function.

The quadrate process (QUP) is very compressed and is flat on both lingual and labial sides (Figures 5a, 6a,b and 9a,b). It develops three unique structures. Firstly, there is an anterior protruding triangular one that is herein named 'proquadrate process' (PQP, new structure), and there are two that are located at the upper rim of the posterior slope of the quadrate process. They are herein named the '*Pronator* process of the palatoquadrate' (PPP, new structure) and the '*Levator palatoquadrati* process alpha' (LPPae, new structure; Figures 5a, 6a,b and 7d,e). Hemigaleids, carcharhinoids and sphyrnids develop a *Levator palatoquadrati* process (LPP) that is located on the lingual surface of the quadrate

FIGURE 7 (a) Lateral left view of the cephalic musculature of *Hemipristis elongata*. (1787-mm TL specimen). ADI, *Adductor mandibularis internus*; CHD, *Constrictor hyoideus dorsalis*; CHV, *Constrictor hyoideus ventralis*; EP, *Epaxial*; EY, eye; HY, hyomandibula; IMD, *Intermandibularis*; LEM, *Levator mandibularis*; LH, *Levator hyomandibularis*; LP, *Levator palatoquadrati*; LPB, *Levator palpebralis*; LPS, *Levator palatoquadrati* superficial sheet; MC, Meckel's cartilage; MER, median raphe; POD, dorsal *Preorbitalis*; POV, ventral *Preorbitalis*; QD, *Quadratomandibularis dorsalis*; QV, *Quadratomandibularis ventralis*; REC, *Rectus*. Scale bar is 4 cm. Drawing A.C. (b) Ventral view of the cephalic musculature of *Hemipristis elongata*. (1787-mm TL specimen). CHV, *Constrictor hyoideus ventralis*; CR, chondrocranium; EY, eye; IMD; *Intermandibularis*; LLC, lower labial cartilage; MC; Meckel's cartilage; POD, dorsal *Preorbitalis*; POV, ventral *Preorbitalis*; POVh, hole in the ventral *Preorbitalis*; PQ, palatoquadrate; QD, *Quadratomandibularis dorsalis*; QV, *Quadratomandibularis ventralis*; ULC, upper labial cartilage; VEF, ventral fascia. Scale bar is 4 cm. Drawing A.C. (c) Dorsal view of the cephalic musculature of *Hemipristis elongata*. (1787-mm TL specimen). ADI, *Adductor mandibularis internus*; CHD, *Constrictor hyoideus dorsalis*; CR, chondrocranium; EP, *Epaxial*; EY, eye; LH, *Levator hyomandibularis*; LP, *Levator palatoquadrati*; LPB, *Levator palpebralis*; LPS, *Levator palatoquadrati* shallow sheet; OBL, *Obliquus*; PQ, palatoquadrate; PR, preorbital process; PRF, parietal fossa; PT, postorbital process; REC, rectus; RTT, tendon of the *Pronator* subdivision of the *Levator palatoquadrati*. Scale bar is 4 cm. Drawing A.C. (d) Dorsolateral view of the cephalic musculature of *Hemipristis elongata*. (1787-mm TL specimen). ADI, *Adductor mandibularis internus*; CHD, *Constrictor hyoideus dorsalis*; CPC, craniopalatoquadrate cartilage; CPT, chondrocranial-palatoquadrate connective tissue sheet; EY, eye; HY, hyomandibula; LEM, *Levator mandibularis*; LH, *Levator hyomandibularis*; LHPI, hyomandibular-palatoquadrate ligament; LP, *Levator palatoquadrati*; LPB, *Levator palpebralis*; LPPae, *Levator palatoquadrati* process alpha, NC, nasal capsule; POD, dorsal *Preorbitalis*; POV, ventral Preorbitalis; PR, preorbital process; QD1, Quadratomandibularis dorsalis division 1; QD2, *Quadratomandibularis dorsalis* division 2; QD3, *Quadratomandibularis dorsalis* division 3; QV, *Quadratomandibularis ventralis*; ROP, *Pronator* subdivision of the *Levator palatoquadrati*; RTT, tendon of the *Pronator* subdivision of the *Levator palatoquadrati*. Scale bar is 4 cm. Drawing A.C. (e) Dorsolateral view of the cephalic musculature of *Hemipristis elongata*. (1787-mm TL specimen). ADI, *Adductor mandibularis internus*; CHD, *Constrictor hyoideus dorsalis*; CPC, craniopalatoquadrate cartilage; CPT, chondrocranial-palatoquadrate connective tissue sheet; EY, eye; HY, hyomandibula; LEM, *Levator mandibularis*; LH, *Levator hyomandibularis*; LHPI, hyomandibular-palatoquadrate ligament; LP, *Levator palatoquadrati*; LPB, *Levator palpebralis*; LPPae, *Levator palatoquadrati* process alpha, NC, nasal capsule; POD, dorsal *Preorbitalis*; POV, ventral Preorbitalis; PR, preorbital process; QD1, Quadratomandibularis dorsalis division 1; QD2, *Quadratomandibularis dorsalis* division 2; QD3, *Quadratomandibularis dorsalis* division 3; QV, *Quadratomandibularis ventralis*; ROP, *Pronator* subdivision of the *Levator palatoquadrati*; RTT, tendon of the *Pronator* subdivision of the *Levator palatoquadrati*. Scale bar is 4 cm. Picture A.C. (f) Dorsal view of the cephalic skeleton of *Hemipristis elongata* showing the semi-schematic representation of the two subdivisions of the *Levator palatoquadrati* and their insertions on the palatoquadrate. The postorbital process has been removed. Dotted lines represent the *Pronator* subdivision underlying the *Levator palatoquadrati*. This illustration is the dorsal view of Figure 5a. CH, ceratohyal; CR, chondrocranium; HY, hyomandibula; LP, *Levator palatoquadrati*; LPPae, *Levator palatoquadrati* process alpha; ORI, orbitoquadrate ridge; PPP, *Pronator* process of the palatoquadrate; PQ, palatoquadrate; PQP, proquadrate process; ROP, *Pronator* subdivision of the *Levator palatoquadrati*; Drawing A.C

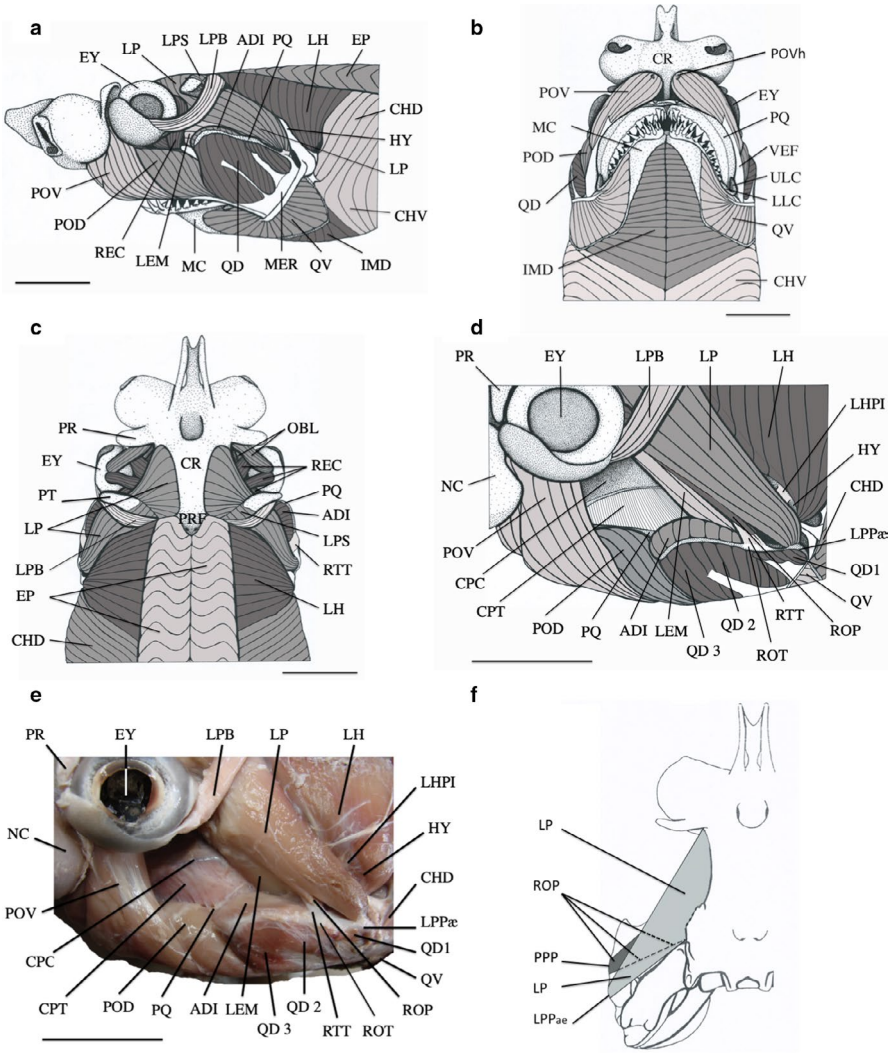

process (Figures 8b,c and 10b,c). *H. elongata* does not develop this process. In all our comparative material, the quadrate process is concave on its lateral/labial surface and convex on its inner/lingual surface.

The quadrate ridge (QR) is only developed as an incipient of a crest at the base of the lateral quadratomandibular joint (DJJ; Figure 5a). This ridge is replaced anterodorsally by a barely distinguishable quadrate fossa (QFO; Figure 5a). The quadrate ridge and fossa are always moderately to strongly developed in our comparative material. These structures offer deeper attachment area for the *Quadratomandibularis dorsalis* in sharks that develop them.

There is a strong orbitoquadrate ridge (ORI; Figure 5a) that runs forward from the quadrate process to reach the orbital process level. This ridge provides an aponeurotic attachment area for the dorsal *Preorbitalis* (POD; see Figures 5a and 7a).

3.3.2 | Meckel's cartilage

The MC exhibits the following relevant features:

The symphysis is very long and dorsally hinged (MSY; Figure 12). The anteromedial end of each MC is septate. Each MC is independent from its antimere and there is a toothless space at the symphysis (Figures 7b, 9a,b and 12). *C. macrostoma* has also a quite long Meckelian symphysis that articulates dorsally as well, but the articulation develops tooth files. Macrophageous lamnoids except *Alopias* spp. develop a condition similar to *H. elongata* (Shimada, 2002 and present study).

The anterior portion of the Meckelian tooth matrix develops a huge and deep Meckelian dental bulla (MDB). These dental bullae house more than half the tooth files of the lower jaw (Figures 6b and 12). *C. macrostoma* develops only an incipient Meckelian dental bulla. This bulla is absent in *H. microsotoma* and *C. melanopterus*. Macrophageous lamnoid taxa have a Meckelian dental bulla that houses only four tooth files at most (Shimada, 2002; Present study).

The dorsal surface of each dental bulla (MDB) is covered by very calcified tooth fold, herein named 'Calcified Meckelian dental fold'. The tesserae do not recover the portion of the fold lining the symphysis (CDF, new structure; Figures 10a and 12). *C. macrostoma* displays the same calcified fold, which is way much smaller. This structure has never been described before though it was illustrated by Leriche (1938, Figure 4); but without any comments. The ventral surface of the basihyal (BH) rests upon these folds.

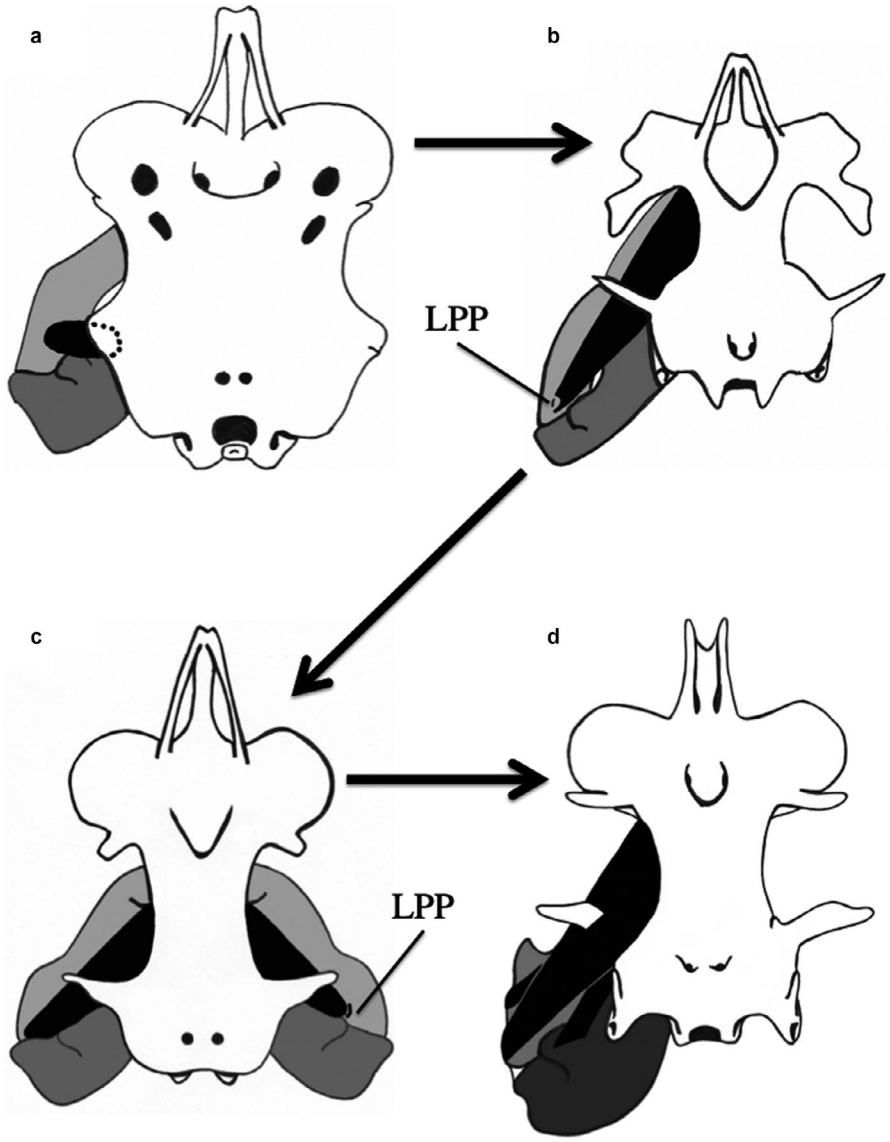

FIGURE 8 Semi-schematic dorsal view of chondrocranium and hyoid arch illustrating a hypothetical morphocline of the *Levator palatoquadrati* (LP) among Carcharhiniformes. A being the most plesiomorphic state and D being the most apomorphic. B and C being intermediate states. (a) condition developed by the more basal families among Carcharhiniformes. (b) condition known in Carcharhinidae and Sphyrnidae. (c) condition developed in *Hemigaleus australiensis*. (d) condition exhibited by *Hemipristis elongata*. Palatoquadrates in light grey, Meckel's cartilages in dark grey, *Levator palatoquadrati* in deep black, chondrocranium in dark outline. LPP, *Levator palatoquadrati* process. Drawing A.C

The ventral rim of the MC forms a strong ridge that runs up to the symphysis level. It fringes the ventral surface of the Meckelian dental bullae. It is herein named 'Meckelian *Intermandibularis* ridge' (MIR, new structure; Figure 6b). It is absent in other hemigaleids, but is developed in many lamnoid taxa (*Carcharias*, *Odontaspis* spp., *Lamna ditropis* (Hubbs and Follett, 1947), *Pseudocarcharias* and *Mitsukurina*; present study).

The lateral quadratomandibular joint (DJJ) is not complete. It does not form an articular joint socket. This quadratomandibular joint is partly replaced by a very compressed and flat ligament (LQL; Figures 5a–c and 6b). At the PQ level the double jaw joint is formed of a lateral quadratomandibular joint condyle that articulates in a deep joint socket of the MC in all other hemigaleids and other higher carcharhinoids. The jaw joint displayed a resistant and firm cohesion in the fresh *H. elongata* skeletonized specimens during hand manipulations.

The Meckelian spine (MES) is very acute and long. It is associated with a deep Meckelian groove (MEG; Figures 5a and 6b). These two structures are not very developed in the other hemigaleids but are well defined in *C. melanopterus*.

3.4 | Description of the hyoid arch

The hyoid arch is composed of a pair of quite stout and quite angular hyomandibulae that display a dorsal surface mildly concave and an underneath one convex (Figures 5a and 6a). Both MCs are a bit longer and thinner than the hyomandibulae (Figure 6a). The BH is shovel shaped and as wide as long (Figure 3b,c).

3.5 | Description of ligaments

3.5.1 | Ethmopalatine ligament (LCP)

In *H. elongata* this ligament has a dual origin on the CR. Anteriorly, it originates from the posterior surface of the ECN. Posteriorly, it originates from the anterior tip of the CPC. The ECN and the SS portions of this ligament converge laterally to the NP and merge.

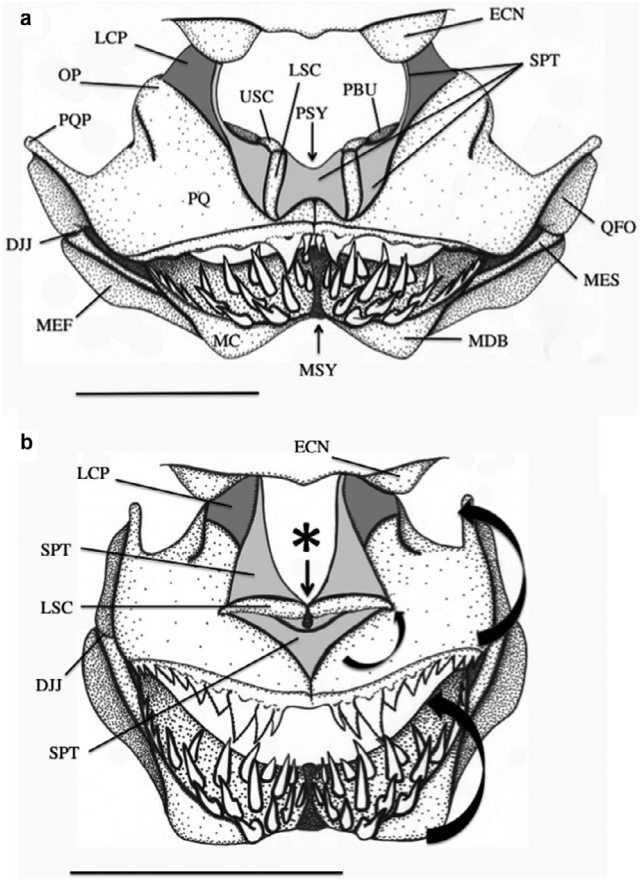

FIGURE 9 (a) Frontal view of the mandibular apparatus of *Hemipristis elongata* in 'resting phase' (1787-mm TL specimen). The mandibular arch has been artificially lowered from the chondrocranium to reveal the suprapalatine cartilages and their arrangement. ECN, ectethmoid condyle; DJJ, double jaw joint; LCP, ethmopalatine ligament; LSC, lower suprapalatine ligament; MC, Meckel's cartilage; MDB, Meckelian dental bulla; MEF, Meckelian fossa; MES, Meckelian spine; MSY, Meckelian symphysis; OP, orbital process; PBU, palatine dental bulla; PQ; palatoquadrate; PQP, proquadrate process; QFO, quadrate fossa; PSY, palatine symphysis; SPT, suprapalatine cartilages connective tissue; USC, upper suprapalatine process. Scale bar is 5 cm. Drawing A.C. (b) Frontal view of the mandibular apparatus of *Hemipristis elongata* (1787-mm TL specimen). The jaws are fully protracted and fully pronated. The asterisk (*) indicates the contact area between the lower suprapalatine cartilages. Upper and lower curved black arrows illustrate the pronation of both palatoquadrates and Meckel's cartilages. ECN, ectethmoid condyle; DJJ, double jaw joint; LCP, ethmopalatine ligament; LSC, lower suprapalatine cartilages; SPT, suprapalatine cartilages connective tissue. Scale bar is 5 cm. Drawing A.C

The resulting single ligament inserts on the dorsal surface of the orbital process. This ligament does not originate from the NP (Figures 4c and 5c). This dual configuration is present in our *H. australiensis*, *C. melanopterus* and *S. lewini* material. It seems it is a feature shared by all carcharhinoids that develop ECNs (unpublished observations). The posterior branch of this ligament originates on the anterior rim of the SS in taxa where the CPC is absent Figures 5b,c, 6a and 9a,b.

3.5.2 | Suprapalatine cartilages connective tissue (SPT)

This connective tissue sheet encompasses the whole SPCs complex and binds it to the palatoquadrate palatine portions dorsal rims. This tissue extends beyond the orbital processes to merge dorsally with the ECN portion of the ethmopalatine ligament (compare Figures 3c and 9a; Figures 3d and 9b). Eventually, it connects to the lower surface of the ECN. In *H. australiensis*, the single pair of SPCs is embedded in a similar connective tissue sheet, yet more lightly developed and confined to the palatine area only (Figure 11b). This connective tissue is absent in *C. melanopterus* and *S. lewini* (Figures 5c and 9a,b).

3.5.3 | Medial hyoid-mandibular ligament (LHMM)

This thick rope-like ligament originates on the lateral rim of the SS, at the posterior end level of the craniopalatoquadrate process. It runs medially to both mandibular and hyoid arches and it inserts on the posterior aspect of the proximal end of the ceratohyal (CH). The dorsal margin of its posterior half is connected to the distal lower surface of the hyomandibula (HY) through a very thin connective sheet. In *H. australiensis*, this ligament has a wide origin below the lateral rim of the SS. It reaches the HY lower surface at its mid-length, and runs against it to eventually insert on the posterior aspect of the CH proximal third. *C. melanopterus* displays a similar configuration to *H. australiensis*. Many lamnoids (Lamnidae, *Carcharias*, *Mitsukurina*) exhibit exactly the same configuration as *H. elongata* (present study) Figure 6a.

3.5.4 | Inner Quadratomandibularis ligament (LQI)

This ligament binds the PQ and its corresponding MC. It originates on the lingual/inner aspect of the quadrate process, runs over the hyomandibular-palatoquadrate ligament (LHPI) to insert on the posteriormost aspect of the mandibular knob. This configuration is similarly arranged in *H. australiensis* and *C. melanopterus* Figure 6a.

3.5.5 | Hyomandibular-palatoquadrate ligament (LHPI)

This wide ligament binds the anterior rim of the distal end of the HY to its corresponding PQ on the lingual surface of the quadrate process. This ligament tapers and runs underneath the inner Quadratomandibularis

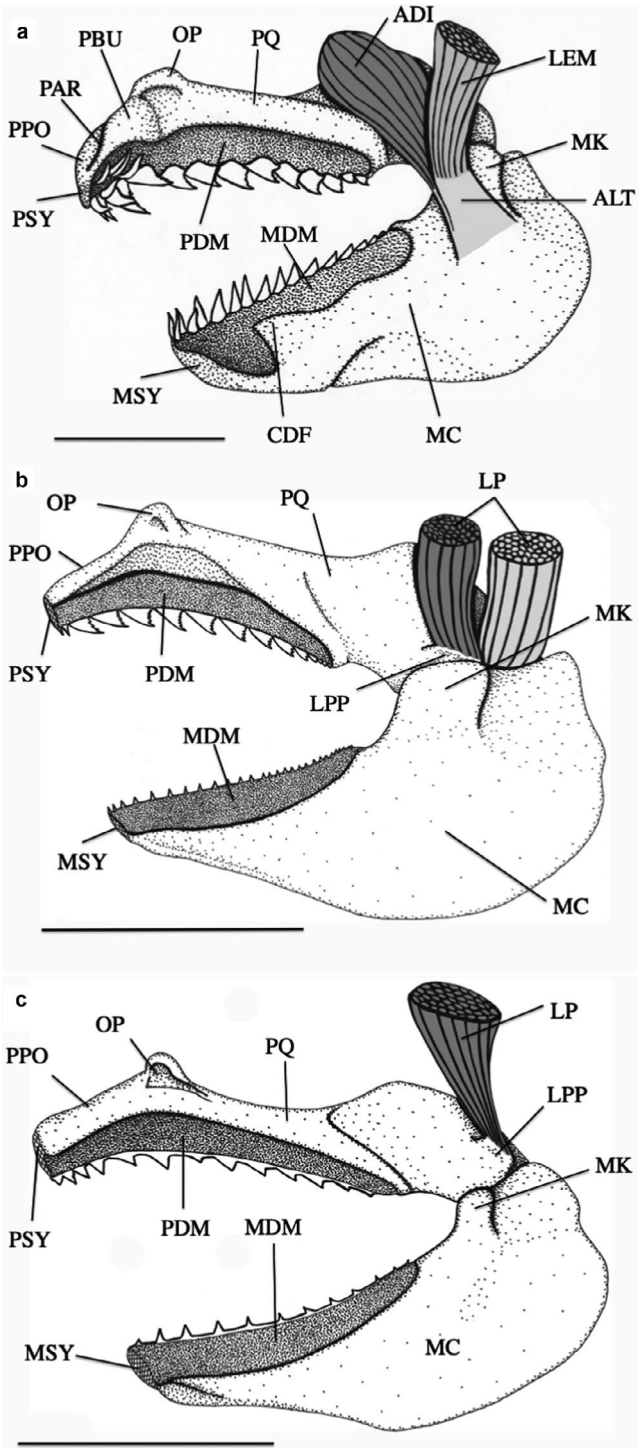

FIGURE 10 (a) Lingual view of the right half of the mandibular arch of *Hemipristis elongata*. ADI, *Adductor mandibularis internus*; ALT, *Adductor mandibularis* and *Levator mandibularis* common tendon; CDF, chondrified Meckelian matrix dental fold; LEM, *Levator mandibularis*; MC, Meckel's cartilage; MDM, Meckelian dental matrix; MK, mandibular knob; MSY, Meckelian symphysis; OP, orbital process; PAR, palatine parasymphyseal ridge; PBU, palatine dental bulla; PDM, palatoquadrate dental matrix; PPO, palatine portion of the palatoquadrate; PQ, palatoquadrate; PSY, palatine symphysis. Scale bar is 5 cm. Drawing A.C. (b) Lingual view of the right half of the mandibular arch of *Hemigaleus australiensis*. LP, *Levator palatoquadrati*; LPP, *Levator palatoquadrati* process; MC, Meckel's cartilage; MDM, Meckelian dental matrix; MK, mandibular knob; MSY, Meckelian symphysis; OP, orbital process; PDM; palatoquadrate dental matrix; PPO, palatine portion of the palatoquadrate; PQ, palatoquadrate; PSY; palatine symphysis. Scale bar is 2 cm. Drawing A.C. (c) Lingual view of the right half of the mandibular arch of *Carcharhinus melanopterus*. LP, *Levator palatoquadrati*; LPP, *Levator palatoquadrati* process; MC, Meckel's cartilage; MDM, Meckelian dental matrix; MK, mandibular knob; MSY, Meckelian symphysis; OP, orbital process; PDM, palatoquadrate dental matrix; PPO, palatine portion of the palatoquadrate; PQ, palatoquadrate; PSY; palatine symphysis. Scale bar is 5 cm. Drawing A.C

ligament (LQl) to insert on a wide surface just behind the PQ tooth matrix. In *H. australiensis* and *C. melanopterus*, this configuration is similar, yet their ligament is more ribbon-like and thinner Figures 5a–c and 6a.

3.5.6 | Lateral quadratomandibularis joint ligament (LQL)

This fan-like ligament is a substitute for the lateral quadratomandibular jaw joint. It binds the PQ and its corresponding MC. This ligamentary configuration is unique to *H. elongata* Figures 5a–c and 6a,b.

3.5.7 | Hyoid-mandibular ligament (LHM)

This ligament binds the lateral proximal end of the CH to its corresponding MC in a depression behind the mandibular knob. The configuration is similar in both *H. australiensis* and *C. melanopterus* Figure 5a–c.

3.6 | Description of the musculature

A great part of the whole cephalic musculature of *H. elongata* complies with those of the higher carcharhinoids in terms of occurrence and arrangement (Compagno, 1988; Wilga, 1995). However, it differs from these sharks by the presence of new muscles and by the shifting of insertion areas of the *Levator palatoquadrati* on the mandibular arch.

3.6.1 | *Preorbitalis* (POD and POV)

This muscle is very large and is divided in two parts: the dorsal *Preorbitalis* (POD) and the ventral *Preorbitalis* (POV). The dorsal *Preorbitalis* displays a pennate outline. It inserts on the lateral base of the orbital process through a tendon. It is quite tightly attached to the labial surface of the orbitoquadrate ridge (ORI) through connective tissue. The ventral *Preorbitalis* (POV) is the longest of the two muscles and is the biggest. It originates on the posterior wall of the nasal capsule (NC) in a wide groove (PVG; Figure 4c) as well

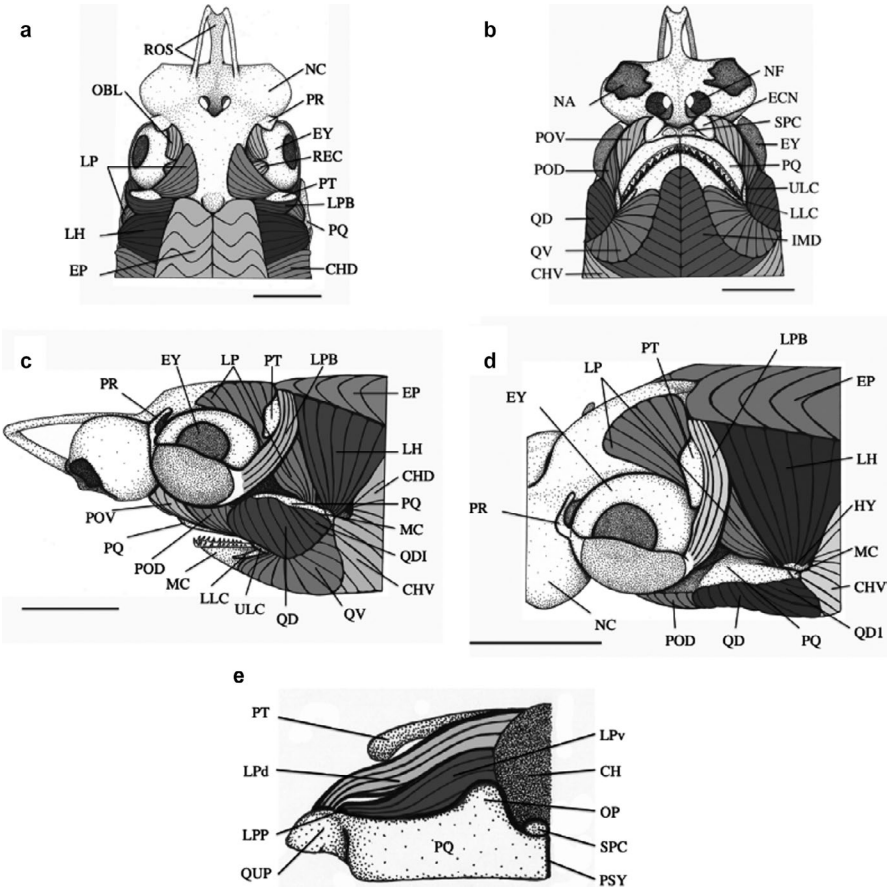

FIGURE 11 (a) Dorsal view of the cephalic musculature of *Hemigaleus australiensis*. CHD, *Constrictor hyoideus dorsalis*; EP, *Epaxial*; EY, eye; LH, *Levator hyomandibularis*; LP, *Levator palatoquadrati*; LPB, *Levator palpebralis*; NC, nasal capsule; OBL, *Obliquus*; PR, preorbital process; PT postorbital process; PQ, palatoquadrate; REC, *Rectus*; ROS, rostral cartilage. Scale bar is 2 cm. Drawing A.C. (b) Ventral view of the cephalic musculature of *Hemigaleus australiensis*. CHV, *Constrictor hyoideus ventralis*; ECN, ectethmoid condyle; EY, eye; IMD, *Intermandibularis*; LLC, lower labial cartilage; NA, nasal aperture; NF, nasal fontanelle; POD, dorsal *Preorbitalis*; POV, ventral *Preorbitalis*; PQ, palatoquadrate; QD, *Quadratomandibularis dorsalis*; QV, *Quadratomandibularis ventralis*; SPC, suprapalatine cartilage; ULC, upper labial cartilage. Scale bar is 2 cm. Drawing A.C. (c) Lateral left view of the cephalic musculature of *Hemigaleus australiensis*. CHD, *Constrictor hyoideus dorsalis*; CHV, *Constrictor hyoideus ventralis*; EP, *Epaxial*; EY, eye; LH, *Levator hyomandibularis*; LLC, lower labial cartilage; LP, *Levator palatoquadrati*; LPB, *Levator palpebralis*; MC, Meckel's cartilage; POV, ventral *Preorbitalis*; PQ, palatoquadrate; PR, preorbital process; PT, postorbital process; QD, *Quadratomandibularis dorsalis*; QD1, Quadratomandibularis dorsalis division 1; QV, *Quadratomandibularis ventralis*; ULC, upper labial cartilage. Scale bar is 2 cm. Drawing A.C. (d) Dorsolateral left view of the cephalic musculature of *Hemigaleus australiensis*. CHV, *Constrictor hyoideus ventralis*; EP, *Epaxial*; EY, eye; HY, hyomandibula; LH, *Levator hyomandibularis*; LP, *Levator palatoquadrati*; LPB, *Levator palpebralis*; MC, Meckel's cartilage; NC, nasal capsule; PQ, palatoquadrate; PR, preorbital process; POD, dorsal *Preorbitalis*; PT, postorbital process; QD, *Quadratomandibularis dorsalis*; QD1, Quadratomandibularis dorsalis division 1. Scale bar is 2 cm. Drawing A.C. (e) Semi-schematic frontal view of the *Levator palatoquadrati* in *Hemigaleus australiensis* seen from behind the nasal capsules level. CH, chondrocranium; LPd, dorsal bundle of the *Levator palatoquadrati*; LPv, ventral bundle of the *Levator palatoquadrati*; LPP, *Levator palatoquadrati* process; OP, orbital process; PQ, palatoquadrate; PSY, palatine symphysis; PT, postorbital process; QUP, quadrate process; SPC, suprapalatine cartilage. Not scale. Drawing A.C

as on the lower surface of the ECN. It also spreads on the poster-oventral surface of the NC where it conceals the nasal fontanelle (Figures 6b and 7b). A 'hole' on the underside of this muscle (POVh) reflects the lack of muscular fibres attached to the reduced nasal fontanelle located underneath (Figure 7b). Posteriorly, both muscles insert on a common ventral fascia (VEF; Figure 7b) shared with the *Quadratomandibularis* complex. In *H. australiensis* and *C. melanopterus*, the ventral *Preorbitalis* has its origin on the posterior wall of the NC only (Figure 11b,c). In *H. australiensis*, the POD is firmly attached to the PQ via the orbitoquadrate ridge length Figure 7a,b,d and e.

3.6.2 | *Quadratomandibularis* (QD and QV)

This muscle is divided into a PQ portion, the *Quadratomandibularis dorsalis* (QD) and a Meckelian one, the *Quadratomandibularis ventralis* (QV). Both are separated by an oblique median raphe (MER; Figure 7a). The *Quadratomandibularis dorsalis* is composed of four Divisions *in H. elongata* (Figure 7a,b,d,e):

The Division QD4 is the deepest one (not illustrated, see Motta and Wilga, 1995; p. 323 for an overview of its position on *N. brevirostris* jaws). It originates on the almost complete quadrate

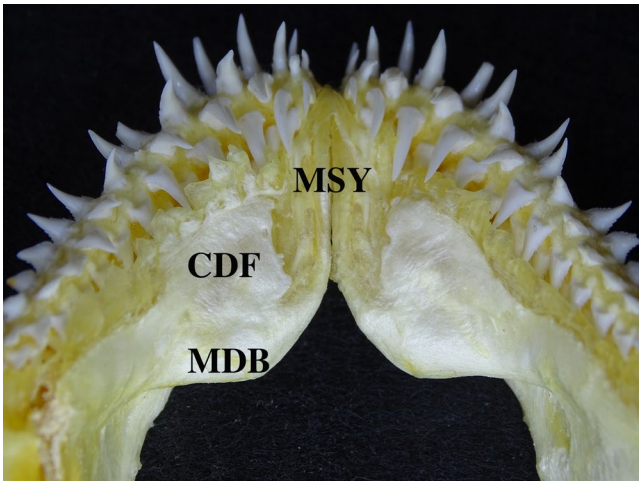

FIGURE 12 Occlusal view of the chondrified Meckelian dental folds in the lower jaw of *Hemipristis elongata* (uncatalogued specimen). CDF, chondrified Meckelian matrix dental fold; MDB, Meckelian dental bulla; MSY, Meckelian symphysis. Photo A.C.

process (QUP) except for the area dorsoposteriorly to the shallow quadrate fossa (QFO). This area is occupied by Division QD1. The proquadrate process (PQP) is not involved in the QD4. It inserts in the deep Meckelian groove (MEG). It does not differ in colour from the three remaining Divisions and is not restricted to the angle of the mouth.

Division QD3 covers up Division QD4 and conceals it completely (Figure 7d,e). A very short tendon attaches this Division to the very anterior end of the proquadrate process (PQP) it mostly covers. Division QD3 is separated from QD4 by the mandibular branch of the trigeminal nerve anteriorly.

Division QD2 is confined to the dorsal half of the *Quadratomandibularis dorsalis* complex between a narrow fascia and Division QD3 ventrally and Division QD1 posterodorsaly (Figure 7d,e). Its dorsal surface originates on the outer rim of the *Pronator* process of the palatoquadrate (PPP). Its lower end inserts on the MER.

Division QD1 is the smallest and the most superficial one (Figure 7d,e). Its anterior end variably recovers some fibres of QD2. Though minute, QD1 seems to be functional since it has its insertion onto the lateral surface of the Meckelian spine summit.

The *Quadratomandibularis ventralis* (QV) consists only of one undivided bundle and is housed in the Meckelian fossa (MEF; Figure 7a,b). It is linked posterodorsally to the *Quadratomandibularis dorsalis* through an insertion on the MER (Figure 7a). *N. brevirostris* develops some QD1 and QD2 of comparable sizes, the former covering the latter entirely (Motta and Wilga, 1995). Its QD4 is confined to the very angle of the jaw and does not extend upward on the quadrate fossa. The *H. australiensis* QD1 is smaller than in *N. brevirostris* and is confined to the rear of the quadrate process (Figure 11c,d). It is more strongly built than in *H. elongata*, though. In *H. australiensis*, it is difficult to distinguish QD2 from QD3, and QD4 seems to be confined to the angle of the jaw as in *N. brevirostris*. (Figure 11b–d).

3.6.3 | *Adductor mandibularis internus* (ADI; new muscle)

This muscle exclusively occurs on the lingual/inner flat surface of the quadrate process (ADF; Figure 6a). It does not extent posterior to the *quadratomandibular* ligament (LQI; Figure 6a). The proquadrate process (PQP) provides an extended origin area. This muscle originates from the complete surface of the ADF and tapers posteroventrally to insert precisely on the median aspect of the mandibular knob (MK) of the MC ahead the inner Quadratomandibularis ligament (LQI) via a wide tendon (ALT; Figure 10a). This tendon is shared with the *Levator mandibularis* (LEM, new muscle; Figure 10a). No other shark is known to develop *adductor* muscles on the lingual/inner facet of the mandibular arch. Batoid Genera *Rhinoptera* and *Gymnura* develop an *Adductor mandibulae lingualis*. This muscle differs in topography from the ADI *of H. elongata* by its extension across both upper and lower jaws (Kolmann et al., 2014; Kolmann et al., 2015) (Figures 7a, c,d,e and 10a).

3.6.4 | *Levator palatoquadrati* (LP, including a subdivision and a new muscle)

The *Levator palatoquadrati* (LP) is a muscle whose origin mainly occurs on the lateral wall of the orbit (OR) as well as on the lateral portion of the CR roof (Figure 7c). Its anterior fibres almost reach the preorbital process level (PR; Figure 7c). As it tapers lateroposteriorly, its fibres go around the *Rectus* muscles complex (REC; Figure 7c) dorsally as well as posteriorly. Some fibres of this muscle originate also from both the ventral and dorsal surfaces of the proximal half of the PT (LPS; Figure 7c). The ECP (Figure 4a,c) is involved as an additional attachment area for the shallow sheet of the LP (LPS; Figure 7c) that runs over the PT. Some posterior fibres of the LP within the OR insert on the ECP as well. Past the level of the PT, the shallow sheet of the LP merges with the main bundle of this muscle under the *Levator palpebralis* (LPB) muscle level. The LP splits into two components that eventually insert on three different areas of the mandibular arch (See Figure 8d). The dorsalmost fibres of the dorsal component of the LP, including the shallow PT sheet (LPS; Figure 7c), taper posterolaterally to insert on the dorsal rim of the quadrate process. It inserts onto a convex blunt extension located at the very rear end of the PQ, the *Levator palatoquadrati* process alpha (LPPae; Figures 7d–f and 8d). The deepest fibres of the dorsal component of the LP have a more lateral orientation. They insert onto a convex area of the dorsal rim of the quadrate process at its mid-length (PPP; Figures 5a and 6a) through a very short tendon (RTT; Figure 7d,e). These fibres share a wide common origin with the basic LP within the OR and diverge from it medially at the proquadrate process level. This bundle is considered here to be a subdivision of the LP: and is named the *Pronator* subdivision of the LP (ROP, new structure; Figure 7d–f). In *C. melanopterus*, the LP consists of a single muscular beam originating from the lateral surface of the OR and inserting on a single process on the PQ (LPP; Figures 8b and 10c). In *H. australiensis*, the LP has a single origin on the laterodorsal wall of the OR but at its mid-length

the LP splits horizontally in two bundles that eventually insert on two distinct locations of the PQ. The deepest and ventralmost bundle originates mainly on the orbital wall then inserts on the LPP (LPv; Figures 10b, 11e and right side of the 8c drawing). The dorsal bundle originates mostly on the lateral margins of the CR roof and then inserts on the PQ laterally to the LPP, against the upper rim of the MC lateral quadratomandibularis jaw joint (LPd; Figures 10b, 11e and left side of the 8c drawing) (Figures 7a, c, d, e, f, 8d and 10a).

In *H. elongata*, the deepest and ventralmost component of the LP distinguishes itself from the dorsal component just past the PT level. It runs a descending trajectory between the SS and the PQ. Eventually, it inserts its flat and wide end onto the mandibular knob (MK) median surface through a wide tendon it shares with the ADI. Because of its complete absence of relationships with the PQ, a new name is herein proposed: the *Levator mandibularis* (LEM, new muscle; Figures 7a,d,e, 8d and 10a). Goto, 2001 illustrates a subdivision of the *Levator palatoquadrati* in the Parascylliidae (p.43, fig.51). In the sharks of this family, the dorsal section originates from the lateral lower side of the CR and inserts on the PQ anterior to the Inner *Quadratomandibularis* ligament. The ventral section originates contiguously to the dorsal section on the CR just posterior to it and inserts on the MC posterior to the Inner Quadratomandibularis ligament. The insertion of the LP lower section is topographically different between Parascylliidae and *H. elongata*. Another Orectolobiformes genus, *Chiloscyllium (*Muller and Henle, 1837; Hemiscylliidae), has a subdivision of the *Spiracularis* inserting onto the mandibular knob (Goto, 2001; p. 44, fig. 52). The Parascylliidae are the only other shark known to have a connection between the CR and the MC via a subdivision of the LP. Goto did not give this muscle any specific name despite its neat separation from the dorsal section at its origin on the CR and its exclusive insertion on the lower jaw.

3.6.5 | *Levator hyomandibularis* (LH)

This muscle has a wide origin area on the lateral surface of the *Epaxial* (EP). Its upper anteriormost fibres originate on the lateral surface of the PP. Its posterior fibres merge with the *Constrictor hyoideus dorsalis* (CHD) but at mid-height, both muscles cleave. Its triangular structure tapers ventrally and inserts on the HY dorsal surface, mainly on its distal half. In *H. australiensis*, the *Levator hyomandibularis* inserts exclusively on the HY dorsal surface (Figure 7a,c,d,e, 11c,d).

3.6.6 | *Constrictor hyoideus dorsalis* and *Constrictor hyoideus ventralis* (CHD and CHV)

Dorsally, the CHD muscle originates on the lateral aspect of the *Epaxial* (EP). Ventrally, it inserts on the distal end of the CH as well as on the MC rear margin through a tendon. *H. australiensis* displays a similar pattern (Figure 11c,d). The CHV muscle is continuous with the *Intermandibularis* (IMD) anteriorly. It inserts onto the posterior margin of the MC where it meets the ventral part of the *Constrictor hyoideus dorsalis* CHD). In *H. australiensis*, the CHV inserts on the MC as well (Figure 11c,d) Figures 7a–c and 11b–d.

3.6.7 | *Intermandibularis* (IMD)

This muscle covers the entire throat region between the ventral rims of the MC. Posteriorly, its fibres merge with those of the *Constrictor hyoideus ventralis* (CHV). Anteriorly, it originates on the dental bullae ventral surfaces (MDB), where it is the thickest. Laterally, it originates onto the deep Meckelian *Intermandibularis* ridges (MIR; Figure 6b). In *H. australiensis*, the IMD originates on the ventral rims of the MCs from the symphysis level Figures 7a,b and 11b.

3.6.8 | *Coracomandibularis* (Not illustrated)

The *Coracomandibularis* inserts on the rear margins of the Meckelian dental bullae (MDB) as well as onto shallow depressions located right behind those bullae against the lingual surface of the Meckelian fossa (MEF). A horizontal fascia separates this muscle from the *Intermandibularis* (IMD). The *Coracomandibularis* consists of a single bundle that widens once the level of insertion on the MC is reached.

3.6.9 | *Epaxial* (EP)

The *Epaxial* inserts on the dorsal surface of the CR up to the PT level (PT) origin. It borders the lateral slopes of the parietal fossa (PRF; Figure 7c). Its anteriormost lateral end inserts on the median aspect of the pterotic process (PTP) and its very anterior tip inserts onto the posterior and median surface of the ECP. Its ventral portion is housed inside the posterior deep fossae (EPM; Figure 4b) of the BP; especially into dedicated depressions located behind the efferent hyoidian artery foramens (BPD; Figure 4b). The extensive and deep insertion of the Epaxial on the BP may explain the extreme posterior shifting of the EHF. In *H. australiensis*, the EP inserts on the lingual side of the PP in a similar way Figures 7a,c and 11a,c.

4 | DISCUSSION

Among the Carcharhiniformes, the families Sphyrnidae, Carcharhinidae and Hemigaleidae exhibit a *Levator palatoquadrati* (LP) muscle whose structure and inferred function differ from those of the more basal families of the order (Compagno, 1988; Motta & Wilga, 1995; Motta et al., 1997; Wilga & Motta, 2000; Wilga et al., 2001). The Carcharhiniformes basal families Scyliorhinidae, Proscylliidae, Pseudotriakidae, Leptochariidae and Triakidae exhibit a vertical arrangement of this muscle (Compagno, 1988; Nakaya, 1975). In those taxa, the LP origin occurs at the rear of the OR and its body descends to insert into a dedicated surface or shallow pit located at the rear of the PQ, on its dorsal/lingual surface

(Figure 8a). Within the higher carcharhinoids, the LP shifts its origin area towards the lateral surface of the orbit, eventually invading it in whole (Figure 8b). It even may reach the PRs and NCs in some taxa (Compagno, 1988). The shallow pit on the dorsal surface of the PQ (when present) is replaced by a *Levator palatoquadrati* process for the insertion of this muscle (LPP; Figures 8b,c and 10b,c). The condition of the LP among the basal families of the Carcharhiniformes is similar in form and function to those of Lamniformes, Orectolobiformes, Heterodontiformes and Squalean sharks, with some variations (Compagno, 1988; Goto, 2001; Huber et al., 2005; Wilga, 2005; Wilga & Motta, 1998b; Shirai, 1992; Soares & Carvalho, 2013). The function of the LP in those taxa is to retract upward the PQ and the mandibular arch (Wilga, 2005; Wilga & Motta, 1998b; Wilga et al., 2001). In the Carcharhinidae and the Sphyrnidae, it has been proposed that the main function of the LP was to contribute to the protrusion of the mandibular arch along with other cranial muscles (*Preorbitalis* and *Quadratomandibularis* muscle complexes, Wilga et al., 2001). Experiments with *N. brevirostris and S. tiburo* show this muscle triggers concomitantly with the onset of jaw protrusion (Motta et al., 1997 and Wilga et al., 2000).

In *H. elongata*, the origin area of the LP is the same as in the other higher carcharhinoids, but its insertion is multiple on the areas of hitherto undescribed parts of the PQ and the MC (Figures 7d,f, 8d and 10a) instead of single in the other carcharhinoids. The dorsal component of the LP inserts exclusively on the dorsal rim of the quadrate process and the *Levator palatoquadrati* process (LPP) for the insertion of this muscle nearby the jaw joint is absent in *H. elongata*. This arrangement led us to wonder how this unique configuration could confer a different jaw kinematic on the snaggletooth shark mandibular arch compared to other higher carcharhinoids.

During the manipulation of the three *H. elongata* heads, we noticed that the jaws readily and smoothly pronate under minimum hand pressure, whatever the steps of preparation. In the *H. australiensis* and *C. melanopterus* specimens, such pronation did not occur by hand manipulations. To quantify these observations, the *H. elongata* skeletonized specimens were placed flat on a plane surface in a configuration similar to the resting phase of the bite (Motta et al., 1997 and Nakaya et al., 2016). Considered from front view, the rostral portions of the quadrate processes were oriented to 62-69 degrees from the PQs occlusal plane. They reach up to 105 degrees when complete pronation was achieved by gentle hand manipulation (Figures 3 and 9a,b). If this rotation of the mandibular arch is so easily performed and so extensive in *H. elongata*, we wonder if some muscles could be directly involved into that process. These results lead us to think that the upper components of the LP are mainly responsible for the lateral rotation of the ventral rim of the upper jaw through the two insertion areas of this muscle. According to the fibre orientation of the *Pronator subdivision* of the LP from its origin on the CR to its insertion area on the palatoquadrate (PPP), this muscle is thought to be solely involved in pulling the quadrate process medially; making the pronation of the PQ possible (Figures 7d–f, and 8d). The orientation of the LP fibres from its origin to the *Levator palatoquadrati* process alpha (LPPae) indicates this muscle may pull the quadrate process towards the anterior area of the OR when the posterior portion of the mandibular arch is depressed. This depression is mechanically resulting from both the lower jaw and lower hyoid arches abduction that eventually induce hyomandibulae depression (Figure 5a,b). Therefore this muscle could be responsible for both the pronation and protrusion of the mandibular arch according to Motta et al.'s hypothesis (1997). The unique addition of a shallow sheet of the LP could provide supplementary muscular force to this muscle during its activity (LPS; Figure 7a,c). Therefore, we suggest both the LP and *Pronator subdivision* of the *Levator palatoquadrati* contribute to the pronation of the upper jaw, and through the double jaw joint, to the pronation of the lower jaw as well. The overall condition of the quadrate process in *H. elongata*, that is, flat and compressed, is thought to be related to the shifting of the LP and the *Pronator subdivision* of the *Levator palatoquadrati* insertions exclusively on its dorsal rim. The straightening of the quadrate process would result from the strains these muscles are supposed to perform there.

The pronation of the mandibular arch is initiated in a joint way through the double jaw joint articulation by the abduction of the lower jaw (Frazetta, 1994; Cf. Figure 3a,b). The quadrate process pronates from 62-69 degrees to about 80 degrees in the three articulated skulls when the MC is lowered by hand manipulation down to its articular limit in *H. elongata*. The same manipulation has been performed on the 1787-mm TL specimen jaw excised from the rest of its cranial skeleton. The amplitude of pronation obtained fell well into the range of the three complete skulls. This result suggests the hyoid arch has little to no effect on the pronation during abduction of the mandibular and hyoid arches. It should be noted that the upper and lower jaws cannot pronate independently of one another; the whole mandibular arch pronates as a unit (Figures 3 and 9a,b). The pronation induced at articular level does not occur or is negligible in *H. australiensis* and *C. melanopterus*. It has been observed in some lamnoid species (*L. nasus*, *I. oxyrinchus*, *C. taurus* and *M. owstoni*; pers. observations). This pronation of the PQs and MCs is only possible due to the condition of both symphyses in *H. elongata*. The Meckelian symphysis is dorsal and long and the palatine one is ventral and short. In *H. australiensis* and *C. melanopterus*, the lower symphysis is ventral and short and the upper is rather vertically arranged. In *H. elongata* the PSY is flanked by a pair of unique structures; the SPCs (USCs and LSCs; Figures 3, 5a and 9a,b). During hand manipulations, we verified that once the pronation of the upper jaw was completed and gone along with its peak protrusion, the bifid ethmopalatine ligaments tauten as do the SPCs connective tissue (SPT; Figures 5c and 9a,b). This connective tissue forces the LSCs to rotate outward to eventually cause their proximal ends to interfere between the palatine portions of the PQs. The USCs always remain tightly attached to the palatine parasymphyseal ridges (USC and PAR; Figures 9a and 10a). The SPC complex is thought to act like some cushion structures preventing possible damages to the palatine portions during pronation when those latter collide (Figure 9b, asterisk and Figure 3d). The rotation and interference of the SPCs between the PQs occurs only and always during maximum protrusion and maximum pronation of the PQs when induced by hand manipulation. This result indicates that these events occur very probably concomitantly during the

biting process, that is, during compressive/protruding phase of jaws in live specimens (suggested by Frazzetta, 1994, p.46).

As the pronation of the upper jaw is achieved, the distance between the orbital processes'lateral margins is reduced to about 28 to 37% from the situation identical to the resting phase (Figures 3 and 9a,b). *Hemipristis elongata* develops long and supple CPC (Figures 4b,c, 5b,c, and 7d,e). These cartilages readily bend anteromedially during hand manipulation of the PQs, especially when pronation and protrusion were performed. They provide further support to the anterior PQ from the suborbital shelves during pronation and protrusion when the orbital processes get closer to each other.

The other main modification of the *Levator palatoquadrati* in *H. elongata* involves its lower component. This muscular bundle inserts exclusively on the MC, onto the mandibular knob (Figure 10a). This newly described muscle, the *Levator mandibularis*, is thought to be involved in the adduction of the jaw (LEM; Figures 7a,d,e, 8d and 10a). Once the jaws closed, this muscle is thought to be also involved in the dorsal retraction of the whole mandibular arch against the CR, assisting the *Levator hyomandibularis* in that task (Motta, 1997). Among the group of mandibular muscles involved in adduction: QV, multiple bodies of QD, POD and POV (Motta et al., 1997; Wilga & Motta, 2000), the QV is the most powerful instead the QD is less powerful as smaller (Huber et al., 2006; Mara et al., 2009; Wroe et al., 2008). We assume that the QD complex of *H. elongata* is relatively shallower than in *H. australiensis* and *C. melanopterus* because of the compressed and straightened anatomy of its quadrate process and the absence of a marked developed quadrate ridge. Yet, the QV does not differ in topography, extension and depth between *H. elongata* and both *H. australiensis* and *C. melanopterus*. Considering the QV is supposed to develop most of the muscular strength leading to jaw adduction and that the ADI is supposed to palliate the reduction of depth of the QD muscles complex, one could wonder if the development of the LEM would not be redundant if we consider its supposed function as being merely a jaw adductor. According to its topographic situation, its origin and insertion areas, the main function of the LEM is to retract the MC towards the CR. This upward retraction would in fact incidentally lead to its adduction against the PQs. In some lamnoids, including *C. Carcharias*, the *Levator hyomandibularis* develops additional insertion areas on the posterior third of the PQ as well as on the MC in the surrounding area of the double jaw joint (Wilga, 2005). This peculiar condition is thought to be related to the multiple protrusion–retraction cycles of the mandibular arch in the course of the white shark feeding behaviour (Tricas & Mc cosker, 1984). In addition to retracting the hyoid arch, the LH would assist the LP in the repetitive retractions of the great white upper jaw during the bite. This novel insertion of the LH on the MC would indicate the retraction of the whole mandibular ach is also an important component of the jaw kinematics in sharks that possess it. Likewise, the development of the LEM in *H. elongata* may be indicative of peculiarities and specificities in its jaw kinematics we can only assume without observations in vivo or through electromyographic experiments. Its main function could be similar to the LH in *C. Carcharias*. Multiple and repetitive protrusion–retraction cycles associated with synchronous pronations could be a normal pattern in the biting behaviour of *H. elongata*.

Hemigaleus australiensis shows a somewhat intermediate condition of the LP between *H. elongata* and other higher carcharhinoids observed including *C. melanopterus* (Figures 8c, 10c and 11e). The insertion area of this muscle upon the PQ is bifid. A ventral bundle inserts onto the *Levator palatoquadrati* process (LPP; Figure 10b and right side of the 8c drawing), whereas a dorsal one is located next to it, close to the MC (Figure 10b and left side of the 8c drawing). Goto (2001) estimated that among Orectolobiformes and Outgroups included in his work, the condition of the LP in the Parascylliidae, which displays a direct muscular connection between the CR and the MC, should be considered apomorphic. A dorsoventrally arranged and single muscle originating from the posterior region of the OR and inserting on the posterior area of the PQ is considered an ancestral condition (Goto, 2001; Wilga et al., 2001). Based on these statements, we propose a hypothetic morphocline for the *Levator palatoquadrati* among Carcharhiniformes. In Figure 8, drawing A represents the most plesiomorphic state whose arrangement is consistent with Wilga et al., 2001. Drawing B shows what is considered the apomorphic state until now (Compagno, 1988; Nakaya, 1975; Wilga et al., 2001). The drawing C represents a step further from state B with the division of the LP and its dual insertions on the PQ. Finally, drawing D would represent the most apomorphic state in which the LP splits into three beams that insert on three different areas, one of which occurring on the MC. Drawing C should be considered the intermediate state between A and B according to Nakaya (1975; p. 71, fig. 34 g), but the novel find regarding the LP bifid condition and its double insertion on the PQ in *H. australiensis* would place it in between the states illustrated by Figure 3b,d.

The most noticeable addition to the cephalic muscular complex of *H. elongata* is the presence of an entire new muscle. The ADI is a muscle exclusively located on the inner surface of the quadrate process which displays the proquadrate process to house it (PQP; Figures 5a and 6a,b). This muscle is thought to be exclusively a jaw adductor (ADI; Figures 7c,d,e and 10a). In addition to their jaw adductor muscle battery, the Batoid genera *Rhinoptera and Gymnura* develop a unique additional muscle located on the lingual face of both jaws; the *Adductor mandibulae lingualis*. Among the six muscles involved in adduction of *R. bonasus* jaws, this muscle is the fourth relative to theoretical force developed (Kolmann et al., 2015). The involvement of the ADI to the muscular complex responsible for adduction in *H. elongata* should not be negligible in that regard. In *Rhinoptera bonasus*, the *Adductor mandibulae lingualis* is considered a possible extension of a widely present muscle in batoid: the *Adductor mandibulae deep*, 'perhaps giving the more dorsoventrally compressed jaws in this genus compared to sister Myliobatids' (Kolmann et al., 2014). Likewise, the unique location of the ADI on the lingual/inner face of the quadrate process could have had an effect on its unique compressed and straightened morphology in *H. elongata*. Since both the *Levator mandibularis* and ADI share the same tendon on the mandibular knob, this suggests the latter could be derived from the former.

The lateral quadratomandibular joint is absent in *H. elongata* and is replaced by a strong and thick lateral quadratomandibular joint ligament (LQL; Figures 5a,b,c and 6b). The absence of this articulation allows a high vertical gape of the mandibular arch. It reaches up to 135 degrees in the 1260-mm TL *H. elongata* skeletonized specimen (110° in the 1787 mm-TL specimen and 119° in the 1920-mm TL specimen), whereas it attains 90° in *H. australiensis* and a bit less than 90° in *C. melanopterus*. It is possible that the absence of the lateral quadratomandibular joint is related to the peculiar compressed and straightened anatomy of the quadrate process.

The muscles involved in the adduction of the jaws in *H. elongata* are the *Quadratomandibularis dorsalis*, the *Quadratomandibularis Ventralis*, the *Preorbitalis ventralis*, the *Preorbitalis dorsalis* (Motta et al., 1997), the new *Levator mandibularis* and the new ADI. Additionally to two new muscles dedicated to this function, one should note the ventral *Preorbitalis* muscle is more developed than in the other higher carcharhinoids (Compagno, 1998; present study). The ventral *Preorbitalis* origin is not restricted to the area between the ECN and the NC as in other Sphyrnidae, Carcharhinidae and Hemigaleidae, but covers entirely the ventral surface of the ECN as well as the posterior portion of the NC (Figure 7a,b). The development of a high and strong subethmoid keel (SK) may be an associated structure that could act as a strut preventing the anterior part of the CR from bending downward during the ventral *Preorbitalis* triggering (Figures 4b,c, 6b and 7b).

The mandibular arch in sharks consists of a complex of four basic elements that can articulate with each other more or less freely, depending on the taxa. The jaws can open and close through their double jaw joints and their abduction is limited by those joints, the *Quadratomandibularis* muscles complex as well as by the labial cartilages. They also perform lateral and medial translations through their upper and lower symphyseal articulations that are induced and limited by the hyoid arch articular range (Nakaya et al., 2008; Scott, 2016; Wu, 1994). Some species can also perform vertical translation between PQs via the symphysis (*Hexanchus griseus*; Bonnaterre, 1788; Pers. observations). Also, each PQs and MCs can rotate along their symphyseal-double jaw joint longitudinal axis, either in pronation and/or supination (Frazetta, 1994; Ramsay & Wilga, 2007; Scott, 2016). Pronation of the mandibular arch is not a feature confined to *H. elongata* only. Many lamnoids pronate their jaws during the bite cycle. Manipulation of thawed or fresh *I. oxyrinchus*, *C. taurus and M. owstoni* specimens demonstrated that their jaws, and especially the PQs, strongly pronate under minimum hand pressure (pers. observations). The pronation allows their upper anterior tooth files to turn maximally erect and functional. Similarities between *H. elongata* and many lamnoids go further. Both have their suborbital shelves (SS) lateroventrally arched with strong BPD (present at least in *Lamna* and *Isurus)*. Both *H. elongata* and many Lamniformes have a developed BPK, strong PP, palatine and Meckelian dental bullae (PBU and MDB), septate upper and lower symphyses articulating ventrally for the upper and dorsally for the lower. *Hemipristis elongata* is the carcharhinoid closest to lamnoids in many aspects (Compagno, 1988; Compagno, 1990 and present study). These anatomical and biomechanical similarities between *H. elongata* and many Lamniformes are either the result of a convergent feeding ecology or long conserved symplesiomorphic characters. Yet, *H. elongata* differs markedly from Lamniformes in the shape and arrangement of its upper teeth. The upper dentition of *H. elongata* indicates it most probably acts like a saw. Higher carcharhinoids with wide upper serrated teeth arranged in imbricated/overlapped fashion (Compagno, 1988) use vigorous and repetitive lateral motions of their head to optimize the cutting effect of the dentition (Frazzetta, 1994; Moss, 1972; Motta et al., 1997; Motta and Wilga, 2001). Processing prey items must be facilitated when the teeth responsible for cutting are positioned on pronated jaws. Pronation of the upper jaws would lead to an outward rotation of the upper teeth (Frazetta, 1994). The outward rotary of the upper tooth battery induced by pronation could be enhanced by the protrusion of the upper jaw. Protrusion and adduction of the PQs would produce a tension at the level of the chondrocranial-palatoquadrate connective tissue sheet (CPT; Figure 7d,e). This tension communicated to the dental ligament would eventually help in erecting the teeth in a more firm and rigid fashion during prey processing (Ramsay & Wilga, 2007). Most macrophageous lamniformes possess narrow and awl-shaped smooth-edged teeth arranged in independent files on multiple functional rows (Shimada, 2002 and present study). The lamnoid upper anterior dentition particularly, once the jaws pronated, is optimized to grasp and hook prey items, preventing them to escape prior to be swallowed in whole (Lucifora et al., 2001). Scott (2016) depicts a cycle of pronation and supination of the mandibular arch in an Orectolobiformes: the white-spotted bamboo shark, *Chiloscyllium plagiosum* (Bennett, 1830). During its biting kinematics, the PQs of *C. plagiosum* pronate to a maximum of 11.4 - 13.2 degrees when the pronation reaches a maximum of 36 - 43 degrees in *Hemipristis elongata*. In *C. plagiosum*, pronation occurs only in jaw adduction and protrusion whereas it already occurs in abduction in *H. elongata* to eventually be completed by adduction. *Chiloscyllium plagiosum* supinates its jaws but this cannot be achieved in *H. elongata* since the articular limits are already reached at resting phase and therefore only pronation is possible. Note that *C. plagiosum* develops a branch of the *Spiracularis* inserting on the mandibular knob (Goto, 2001). This muscular derivation might have a relation with supination abilities in that species. *Hemipristis elongata* mandibular arch is thought to retrieve its situation similar to the resting phase by the involvement of the unusually thick *Intermandibularis* muscle and its origins onto the Meckelian *Intermandibularis* ridges (Figure 6b). These differences in jaw kinematics reflect the differences in lineages as well as in food diets, behaviours and habitats (benthic vs benthopelagic) between those two species. *Chiloscyllium plagiosum* is variably a crushing or clutching toothed shark that is most unable to sever or gouge its preys. Moreover, its feeding behaviour relies mainly on suction capture. Its mouth is small, flanked with strong labial folds complex and its dentition is small and virtually homodont on both jaws (Ramsey & Wilga, 2007). *Hemipristis elongata* differs in having large teeth displayed along the jaws with a strong dignathic heterodonty. Its mouth is

well cleft posteriorly and its labial cartilages and folds are small and barely reduce the mouth gape.

The presence of upper jaw pronation abilities in sharks that distant in terms of phylogeny, feeding behaviour and diet may be indicative of a far more common occurrence among this group of Elasmobranchs as it has been suggested by Frazetta & Prange, 1987 as well as by Wilga et al., 2001 (Present study, unpublished observations). Pronation of the upper jaw allows the upper teeth to be more erect and consequently more efficient during the bite especially when those improve capture (Lamniformes; Frazetta, 1988 and present study) or gouging of the prey items (derived Carcharhiniformes; Frazetta, 1994; Frazetta & Prange, 1987; Moss, 1972; Motta et al., 1997; Motta & Wilga, 2001).

Based on our observations on *H. elongata* and following the hypothesis of Frazetta (1994) who suggested that the pronation of the upper jaw possibly involves the *Levator palatoquadrati*, we infer that the LP in the higher carcharhinoids is not involved in protrusion as hypothesized by Motta et al., 1997 and Wilga et al., 2001, but is a mandibular arch *Pronator* muscle instead. To consider the exclusive involvement of the *Levator palatoquadrati* in jaw protrusion in higher carcharhinoids is unnecessary because sharks that are able to protrude their jaws do not need the derived carcharhinoid LP arrangement to achieve this function (Wilga et al., 2001). In *S. tiburo* and *N. brevirostris*, the LP triggering occurs concomitantly to the onset of the adductor and protrusive jaw muscles activities (Motta et al., 1997 and Wilga et al., 2000). The LP activity associated with jaw protrusion, certified by motor pattern analyses, does not necessarily mean it is responsible for it or even that it participates to it. Within the higher carcharhinoids, the activity of the LP causing the PQs pronation during protrusion could be a biomechanical advantage concomitant to adduction that would lead to the improvement in the processing of prey items (Frazzetta, 1994; Motta and Wilga, 2001).

Our study suggest that the pronation of the mandibular arch and a probable high bite force are basic components of *H. elongata* feeding behaviour. The mandibular arch and the dentition of the snaggletooth shark display exaggerated and exclusive anatomical features. The strongly hooked lower dentition and the large upper and very strongly serrated teeth are both developed by highly enlarged and inflated dental matrixes and bullae. Muscles that are responsible for the closure, retraction and pronation of the jaws are hyper-developed or unique. Strongly developed and unique chondrocranial structures that offer increased muscle insertion areas are present. *Hemipristis elongata* has a diet that does not differ from other sharks of the same size and sharing its habitat. This diet includes bony fishes, *Carcharhinus* spp. and *Gymnura* sp. as well as cephalopods (Ebert et al., 2013; Last et al., 2009; Setna & Sarangdhar, 1949). We assume that the possession and combination of the multiple unique characters related to its chondrocranio-mandibular anatomy confer on *H. elongata* mandibular kinematics advantages to its feeding ecology (Figure 12).

AUTHOR'S CONTRIBUTIONS

Conceptualization: Chappell A. and Séret B. Data curation: Chappell A. Resources: Chappell A. and Séret B. Pictures: Chappell A. and Séret B. Drawings: Chappell A. Writing and editing: Chappell A. Supervision: Séret B. Validation: Chappell A. and Séret B.

ACKNOWLEDGEMENTS

The authors are very grateful to the colleagues who kindly provided the heads of snaggletooth shark: Vincent Lucas (Seychelles fishing Authority: SFA), Laurent Dagorn (IRD & SFA), John Neville (Environment Seychelles), Geremy Cliff (Natal Shark Board, South Africa), and thank the following ones who facilitate their transports: Alain Fonteneau (IRD), Emmanuel Chassot (IRD & SFA) and Steven Surina (Shark Education). Sirachai Arunrugustichai provided pictures and observations of *H. elongata* fished in Thailand. Will White (CSIRO, Hobart) provided heads of other *Hemigaleid* sharks for comparison. Serra Arnaud and Chretiennot Alexandre provided technical assistance. We thank the anonymous reviewers for their remarks which improved this paper.

ORCID

Anthony Chappell https://orcid.org/0000-0003-0797-6973
Bernard Séret https://orcid.org/0000-0003-2029-8740

REFERENCES

Baranes, A. & Ben-Tuvia, A. (1979) Two rare carcharhinids, *Hemipristis elongatus* and *Iago omanensis*, from the northern Red Sea. *Israel Journal of Zoology*, 28, 39–50.

Bass, A.J., D'Aubrey, J.D. & Kistnasamy, N. (1975) Sharks of the east coast of Southern Africa. III. The families Carcharhinidae (excluding Mustelus and Carcharhinus) and Sphyrnidae. South African Association for Marine Biological Research. Oceanographic Research Institute. Investigational Report No 38:1–100.

Bhullar, B.A.S., Manafzadeh, A.R., Miyamae, J.A., Hoffman, E.A., Brainerd, E.L., Musinsky, C. et al. (2019) Rolling of the jaw is essential for mammalian chewing and tribosphenic molar function. *Nature*, 566, 528–533.

Compagno, L.J.V. (1984) FAO Species Catalogue. Vol. 4. Sharks of the World. An Annotated and Illustrated Catalogue of Shark Species Known to Date. Part 2. Carcharhiniformes. FAO Fisheries Synopsis 125 (4, pt. 2): 251–655.

Compagno, L.J.V. (1988) *Sharks of the Order Carcharhiniformes*. Princeton, N.J.Princeton University Press, p. 486.

Compagno, L.J.V. (1990) Relationships of the Megamouth Shark, Megachasma pelagios (Lamniformes: Megachasmidae), with comments on its feeding habits. In: Pratt Jr H.L., Gruber, S.H., Taniuchi T., (Eds.). *Elasmobranchs as Living Resources: Advances in the Biology, Ecology, Systematics, and the Status of the Fisheries. NOAA Tech Rep NMFS 90*. Washington, D.C: National Oceanic and Atmospheric Administration, pp. 357–380.

Ebert, D.A., Fowler, S. & Compagno, L.J.V. (2013) *Sharks of the World. A fully Illustrated guide*: Wild Nature Press, p. 528.

Fourmanoir, P. (1961) Requins de la côte ouest de Madagascar. *Mémoires de l'Institut Scientifique de Madagascar, Série F, Océanographie*, 4, 1–81.

Frazetta, T.H. (1988) The mechanics of cutting and the form of shark teeth (Chondrichthyes, Elasmobranchii. *Zoomorphology*, 108, 93–107.

Frazetta, T.H. (1994) Feeding mechanisms in sharks and other elasmobranchs. *Advances in Comparative and Environmental Physiology*, 18, 31–57.

Frazetta, T.H. & Prange, C.D. (1987) Movements of cephalic components during feeding in some requiem sharks (Carcharhiniformes: Carcharhinidae). *Copeia*, 1987(4), 979–993.

Goto, T. (2001) Comparative anatomy, phylogeny, and cladistic classification of the order Orectolobiformes (Chondrichthyes,

Elasmobranchii). *Memoirs of the Graduate School of Fisheries Science Hokkaido University*, 48, 1–100.

Herman, J., Hovestadt-Euler, M. & Hovestadt, D.C. (2003) Contributions to the study of the comparative morphology of teeth and other relevant ichthyodorulites in living supraspecific taxa of chondrichthyan fishes. Part A: Selachii. Addendum to 1: Order Hexanchiformes-family Hexanchidae, 2: Order Carchahiniformes, 2a: Family Triakidae, 2b: Family Scyliorhinidae, 2c: Family Carcharhinidae; Hemigaleidae, Leptochariidae, Sphyrnidae, Proscylliidae and Pseudotriakidae, 3: Order Squaliformes: Family Echinorhinidae, Oxynotidae and Squalidae. Tooth vascularization and phylogenetic Interpretation. Bulletin de l'Institut Royal des Sciences Naturelles de Belgique. *Biologie*, 73, 5–26.

Huber, D.R., Eason, T.G., Hueter, R.E. & Motta, P.J. (2005) Analysis of the bite force and mechanical design of the feeding mechanism of the durophageous horn shark *Heterodontus francisci*. *The Journal of Experimental Biology*, 208, 3553–3571.

Huber, D.R., Weggelaar, C.L. & Motta, P.J. (2006) Scaling of bite force in the blacktip shark *Carcharhinus limbatus*. *Zoology*, 109, 109–119.

Huber, D.R., Soares, M.C. & de Carvalho, P.R. (2011) Cartilaginous fishes cranial muscles. *Encyclopedia of Fish physiology: From genome to Environment*, 1, 449–462.

Klunzinger, C.B. (1871) Synopsis der Fische des Rothen Meeres. II. Theil. *Verhandlungen der Zoologisch - Botanischen gesellschaft. (Vienna)*, 21, 441–688.

Kolmann, M.A., Huber, D.R., Dean, M.N. & Grubbs, R.D. (2014) Myological variability in a decoupled skeletal system: Batoid cranial anatomy. *Journal of Morphology*, 275, 862–881.

Kolmann, M.A., Huber, D.R., Motta, P.J. & Grubbs, R.D. (2015) Feeding biomechanics of the cownose ray, *Rhinoptera bonasus*, over ontogeny. *Journal of Anatomy*, 227, 341–351.

Last, P.R. & Stevens, J.D. (2009) Sharks and Rays of Australia. *CSIRO Publishing*, 644, pp.

Leriche, M. (1938) Contributions à l'étude des poissons fossiles des pays riverains de la Méditerranée Américaine (Venezuela, Trinité, Antilles, Mexique). *Mémoires de la Société Paléontologique Suisse*, 61(1), 1–42.

Lucifora, L.O., Menni, R.C. & Escalante, A.H. (2001) Analysis of dental insertion angles in the sand tiger shark, *Carcharias taurus* (Chondrichthyes: Lamniformes). *Cybium*, 25(1), 23–31.

Mara, K.R., Motta, P.J. & Huber, D.R. (2009) Bite force and performance in the durophagous bonnethead shark, *Sphyrna tiburo*. *Journal of Experimental Zoology*, 311A, 11.

Moss, S.A. (1972) The feeding mechanism of sharks of the family Carcharhinidae. *Journal of Zoology*. London, 167, 433–436.

Motta, P.J. & Wilga, C.D. (1995) Anatomy of the feeding apparatus of the lemon shark, *Negaprion brevirostris*. *Journal of Morphology*, 226, 309–329.

Motta, P.J., Hueter, R.E. & Tricas, T.C. (1997) Feeding mechanism and functional morphology of the jaws of the lemon shark, *Negaprion brevirostris* (Chondrichthyes, Carcharhinidae). *Journal of Experimental Biology*, 200, 2765–2780.

Motta, P.J. & Huber, D.R. (2012) Prey capture and feeding mechanics of elasmobranchs. In: Biology of sharks and their relatives. Editors, Carrier JC, Musick JA and Heithaus MR. pp: 153–209.

Nakaya, K. (1975) Taxonomy, comparative anatomy and phylogeny of Japanese catsharks. *Scyliorhinidae. Mem. Fac. Fish. Hokkaido Univ*, 23, 1–94.

Nakaya, K., Matsumoto, R. & Suda, K. (2008) Feeding strategy of the Megamouth shark *Megachasma pelagios* (Lamniformes: Megachasmidae). *Journal of Fish Biology*, 2008(73), 17–34.

Nakaya, K., Tomita, T., Suda, K., Sato K., Ogimoto K., Chappell A. et al. (2016) Slingshot feeding of the goblin shark Mitsukurina owstoni. (Pisces: lamniformes: Mitsukurinidae). *Scientific Reports*, 6, 27786. https://doi.org/10.1038/srep27786.

Ramsay, J.B.& Wilga, C.D. (2007) Morphology and mechanics of the teeth and jaws of white-spotted bamboo sharks (*Chiloscyllium plagiosum*). *Journal of Morphology*, 268, 664–682.

Scott, B. (2016) Three-Dimensional kinematics of the jaws and hyoid during feeding in white-spotted bamboo sharks. University of Rhode Island, Open Access master's Theses. *Paper*, 896, 94 p.

Setna, S.B. & Sarangdhar, P.N. (1949) A contribution of the systematics of *Scoliodon acutus* (Rüppell), *Hemipristis elongatus* (Klunzinger) and *Torpedo zugmayeri* (Engelhart). *Records of the Indian Museum*, 47, 127–134.

Shimada, K. (2002) Dental homologies in Lamniform sharks (Chondrichthyes: Elasmobranchii). *Journal of Morphology*, 251, 38–72.

Shirai, S. (1992) *Squalean Phylogeny. A New Framework of « Squaloid » sharks and related taxa*. Sapporo: Hokkaido University Press, p. 151 pp.

Smith, J.L.B. (1957) The rare shark *Hemipristis elongatus* (Klunzinger), 1871, from Zanzibar and Mozambique. *Journal of Natural History*, 10 (115), 555–560.

Soares, M.C. & De Carvalho, M.R. (2013) Mandibular and hyoid muscles of Galeomorph sharks (Chondrichthyes: Elasmobranchii), with remarks on the phylogenetic interrelationships. *Journal of Morphology*, 274, 1111–1123.

Tricas, T.C. & McCosker, J.E. (1984) Predatory behavior of the white shark, Carcharodon Carcharias, with notes on its biology. *Proceedings of the California Academy of Sciences*, 14, 221–238.

Vélez-Zuazo, X. & Agnarsson, I. (2011) Shark tales: A molecular species-level phylogeny of sharks (Selachimorpha, Chondrichthyes). *Molecular Phylogenetics and Evolution*, 58, 207–217.

Wilga, C.D. (2005) Morphology and evolution of the jaw suspension in Lamniform sharks. *Journal of Morphology*, 265, 102–119.

Wilga, C.D. & Motta, P.J. (1998b) Conservation and variation in the feeding mechanism of the spiny dogfish *Squalus acanthias*. *Journal of Experimental Biology*, 201, 1345–1358.

Wilga, C.D. & Motta, P.J. (2000) Durophagy in sharks: Feeding mechanics of the hammerhead Sphyrna tiburo. *The Journal of Experimental biology*, 203, 2781–2796.

Wilga, C.D., Hueter, R.E., Wainwright, P.C. & Motta, P.J. (2001) Evolution of upper jaw protrusion mechanisms in elasmobranchs. *American Zoology*, 41, 1248–1257.

Wroe, S., Huber, D.R., Lowry, M., McHenry, C., Moreno, K. & Clausen, P. (2008) Three-dimensional computer analysis of white shark jaw mechanics: how hard can a great white bite? *Journal of zoology*, 276, 336–342.

Wu, E.H. (1994) Kinematics analysis of jaw protrusion in orectolobiform sharks: A New mechanism for jaw protrusion in elasmobranchs. *Journal of Morphology*, 222, 175–190.

How to cite this article: Chappell A, Séret B. Functional Morphology of the Feeding Apparatus of the Snaggletooth Shark, *Hemipristis elongata* (Carcharhiniformes: Hemigaleidae). *J. Anat*. 2020;00:1–20. https://doi.org/10.1111/joa.13313